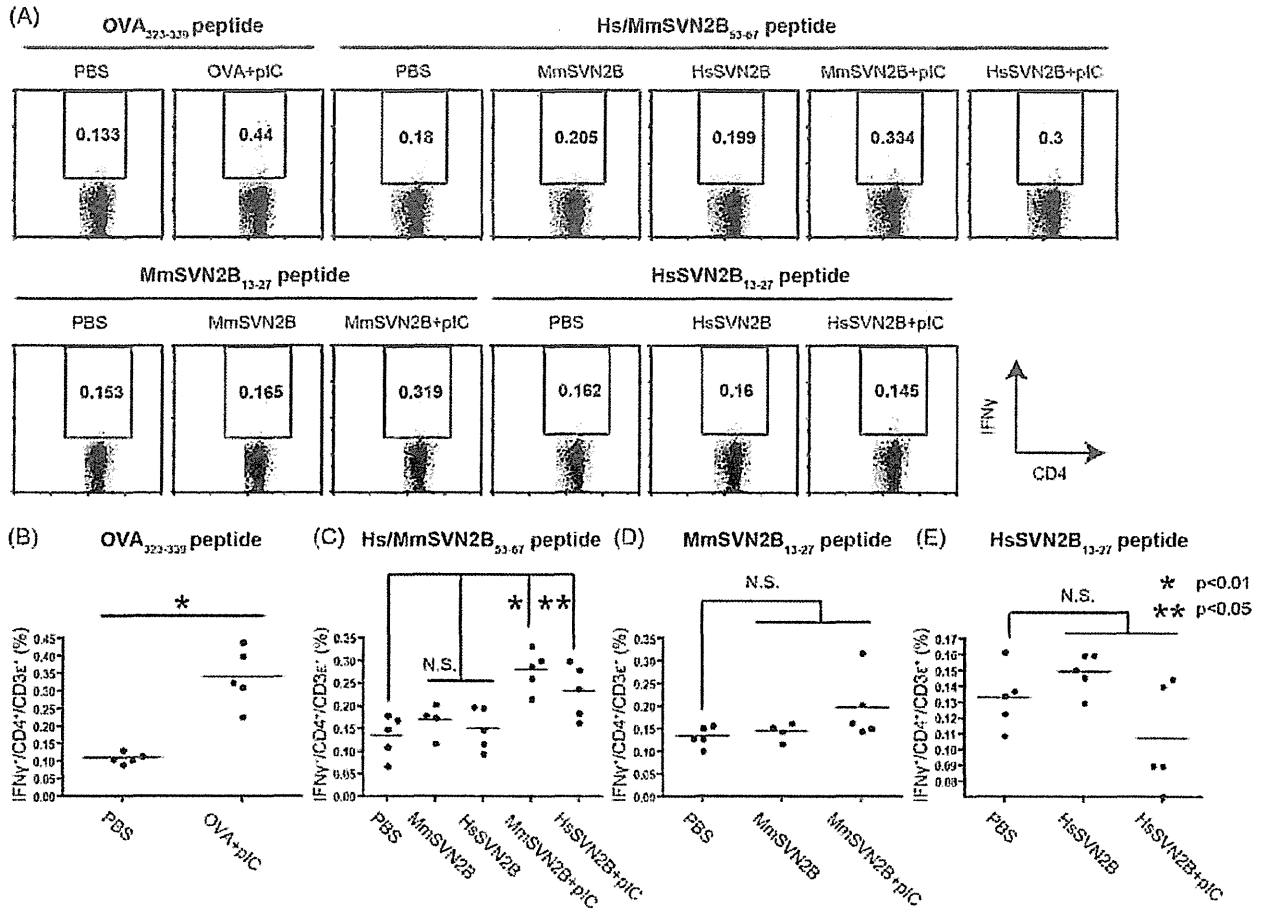

Fig. 4. Expansion of OVA and SVN-specific CD4+ T cells. (A) HLA24b-Tg mice were immunized with 100 μg each antigen and 100 μg poly I:C once a week for 4 weeks. After 7 days from the last immunization, splenocytes were cultured with 100 nM $OVA_{323-339}$ peptide or SVN helper peptide for 6 h, and 10 μg/ml brefeldin A (Sigma–Aldrich) was added in the last 5 h. After cell surface and intracellular staining, IFN-γ production of CD4+ T cells was measured by FACS. Average percentages of IFN-γ-producing CD4+ T cells in response to (B) $OVA_{323-339}$ peptide; (C) Hs/Mm SVN_{53-67} peptide; (D) $MmSVN_{13-27}$ peptide; (E) $HsSVN_{13-27}$ peptide. *$p < 0.01$, **$p < 0.05$.

restimulated with $MmSVN_{13-27}$ or $HsSVN_{13-27}$ peptide (Fig. 4D, E). Differences in these two CD4 epitope sequences are in Fig. 2B.

Ab production by immunization with MmSVN2B with polyI:C

Activation of Th1 cells is essential for B cell antibody class switching. Therefore, we examined production of SVN-specific Ab in Tg mice that did or did not receive polyI:C. Serum was collected from HLA24b-Tg mice immunized with different Ags and polyI:C. OVA and polyI:C were the positive control and resulted in a significant increase in OVA-specific IgG1, IgG2a and IgG2b by ELISA (Fig. 5 left panels). When HLA24b-Tg mice were immunized with MmSVN2B or HsSVN2B without polyI:C, no significant production of any isotypes was observed (Fig. 5 center and right panels). When polyI:C was included, MmSVN2B or HsSVN2B-specific isotypes increased significantly.

Discussion

We demonstrated that HLA24b-Tg mice induced $Hs/MmSVN_{53-67}$-specific CD4+ T cells and SVN-specific Ab followed by Th1 cell activation in response to injection of polyI:C and MmSVN2B protein. This result was partly inconsistent with a previous report (Charalambous et al. 2006) using Balb/c mice and HsSVN conjugated to Dec205 mAb. That is, our study with C57BL/6 mice and MmSVN2B did not detect significant increases in $MmSVN_{13-27}$-specific CD4+ T cells after subcutaneous injection of MmSVN2B with polyI:C. Thus, the xenogeneic differences in sequence between HsSVN and MmSVN did not always contribute to generating effective CD4+ T cells specific for a tumorigenic protein in C57BL/6 mice. The haplotype of the MHC class II proteins between Balb/c (having H-2d) and C57BL/6 mice (having H-2b) and Dec205 mAb conjugation (Charalambous et al. 2006) might be the reason for these different results. However, no CD8+ CTLs against the 2B peptide were detected even when using a specific tetramer for detection of CD8+ CTLs (Fig. S1). Hence, polyI:C was required for proliferation of self-reactive CD4+ Th1 cells that recognized the syngeneic epitope without proliferation of SVN2B peptide-specific CTLs.

OVA were used as positive controls (Fig. 3A, B left panels), and SL8 (SIINFEKL)-specific CTLs were monitored with OVA tetramer (Azuma et al. 2012). Here, T cell activation by polyI:C + MmSVN2B is a focus in this study. However, there is a lot-to-lot difference of T cell-activating activity in polyI:C + OVA as in our present and previous studies (Azuma et al. 2012). This difference of T cell activation may be attributable to the fact that polyI:C consists of a variety of length of polyI chains and polyC chains with a lot-to-lot heterogeneity. In addition, the amounts of Ags in Azuma's experiment are higher than those in the present experiment (Azuma et al. 2012). CD40 stimulation by specific Ab results in high enhancement of cross-priming of CD8 T cells (Charalambous et al. 2006) and CD40 was up-regulated in CD8α+ DCs by polyI:C treatment, but the CD40

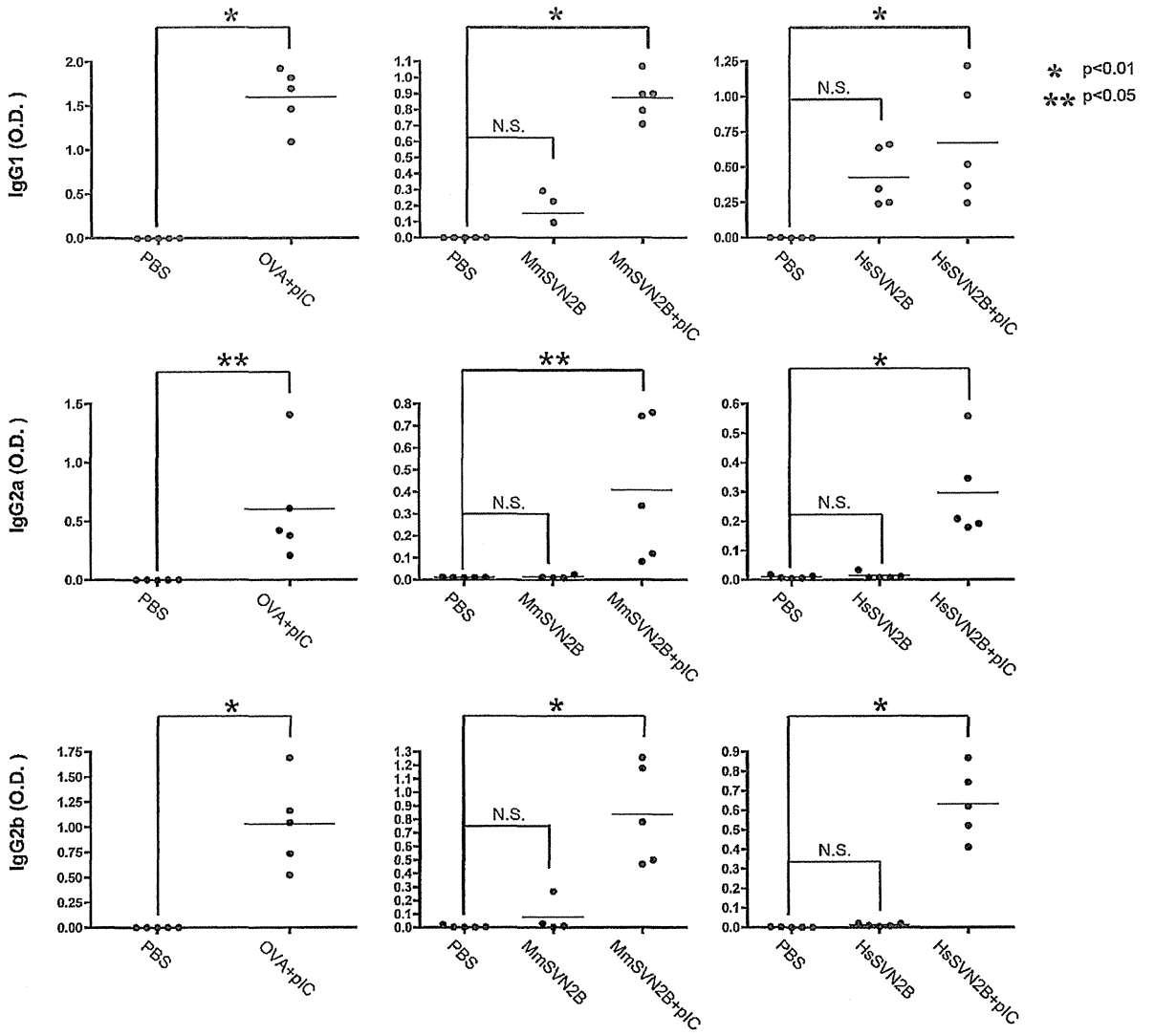

Fig. 5. Production of OVA and SVN-specific antibodies. Sera were collected from immunized mice at once a week for 4 weeks. Anti-OVA or anti-SVN in sera was assessed by ELISA using antiserum for IgG2a/b and IgG1. $^{*}p < 0.01$, $^{**}p < 0.05$.

levels were also variable depending upon the polyI:C lots. Development of a synthesizing method for defined length of RNA duplex will settle the issue.

Two points are noted. First, polyI:C, an RNA adjuvant, induces $CD4^+$ T cells in addition to the reported cases of $CD8^+$ T cells. The factors that participate in polyI:C-mediated CD4+ T cell proliferation and the kind of $CD4^+$ T subsets that are predominantly induced by polyI:C remain unknown. PolyI:C is primarily a potential activator of the IFN-inducing pathways RIG-I/MDA5 and TLR3 (Matsumoto & Seya 2008). These pathways allow host immune cells to produce type I/III IFNs and cytokines and are soluble effectors against cancer. TLR3 preferentially induces cross-presentation in $CD8\alpha^+$ DC in response to dsRNA including polyI:C (Schulz et al., 2005; Azuma et al. 2012) and causes proliferation of $CD8^+$ T cells including cells that respond to TAAs *via* cross-priming (Azuma et al. 2012). $CD4^+$ T cells that are likely evoked by polyI:C stimulation function in antitumor immunity since their helper function is usually suppressed in tumor-bearing mice and can be relieved by innate immune response (Lee et al. 2013). Stimulation with polyI:C + SVN Ag might change a tumor-derived suppressive environment to an environment suitable for primary activation and maintenance of Ag-specific cytotoxic $CD8^+$ T cell responses (Ridge et al. 1998; Janssen et al. 2003).

According to a recent report, however, adoptively transferred $CD4^+$ T cells induce tumor rejection independently of $CD8^+$ T cells (Corthay et al. 2005; Perez-Diez et al. 2007). This rejection is apparently based on cytokines released from $CD4^+$ T cells (Corthay et al. 2005) and on interaction with $CD4^+$ T cells and other immune cells such as macrophages (Mfs) and natural killer (NK) cells (Perez-Diez et al. 2007). DCs stimulated with polyI:C also result in NK cell activation after DC-NK cell-to-cell contact (Akazawa et al. 2007). Mfs in tumors might be a direct target of dsRNA, which converts tumor-supporting Mfs into tumoricidal Mfs (Shime et al. 2012). IL-12p40 is preferentially produced *via* the TICAM-1/Batf3 pathway in response to dsRNA (Azuma et al. 2013). Thus, a variety of cellular effectors can be triggered as antitumor agents by administration of dsRNA with TAA peptides or proteins. We found that $CD4^+$ T cells with Th1 properties were effectors induced by polyI:C possibly acting as an antitumor agent in SVN-responding tumor cells. Although epitope sequence and hydrophobicity might affect Th1 polarization in mice, $CD4^+$ T effectors are successfully induced in tumor-bearing or tumor-implanted mice by stimulation with MmSVN2B + polyI:C.

Hence, *in vivo* administration of an RNA adjuvant with Ag proteins induce $CD4^+$ helper T cells secondary to class II presentation in DCs, together with induction of type I IFNs and cytokines. $CD4^+$ T cells also facilitate Ab production caused by stimulation of B cell development (Mak et al. 2003).

Notably, this is a specific feature of RNA adjuvants, since TLR2 agonist Pam2 lipopeptides such as Pam2CSK4 and MALP2s induce antitumor CTLs with sufficient potential (Chua et al. 2014) but fail to induce DC-mediated antitumor NK cell activation (Yamazaki et al. 2011; Sawahata et al. 2011). $CD4^+$ T cells with regulatory modes such as Tregs and Tr-1 cells and IL-10 were induced by Pam2 peptide in the presence of Ag (Yamazaki et al. 2011). Nevertheless, robust proliferation of antitumor CTL is induced by Pam2 lipopeptides (Chua et al. 2014). Thus, the mode of $CD8^+$ T cell proliferation is differentially modulated between TLR2 and TLR3/MDA5 agonists.

The other point is how self-Ag-reactive $CD4^+$ T cells that act as Th1 effectors in SVN-based immunotherapy are generated. Proliferation of self-reactive T cells is prevented in normal mice, so the levels of self-reactive T cells are usually lower than the detection limit of assays (Gebe et al. 2003). Self-reactive $CD4^+$ T cells might be positively regulated by polyI:C in the presence of protein antigen, since mice, when exposed to DNA/RNA, harbor autoimmune diseases against the protein (Mills 2011). However, even with Ag proteins, polyI:C induced minimal cross-priming of $CD8^+$ T cells in our setting, as with previous reports (Charalambous et al. 2006). In this and other studies, both syngeneic and xenogeneic CD4 epitopes prime $CD4^+$ T cells, stimulating Ab production and Th1 polarization with antitumor activity, but with little association with CTL induction (Charalambous et al. 2006). Our SVN results suggested that self-responsive CD4 epitopes that are identical in sequence in human and mouse SVN have a conserved function as a Th1 skewer, albeit modest, in mice by stimulating DCs and Mfs to prime T and B cells. In this context, however, a question remains to be settled about why the insertion of the 2B sequence in MmSVN caused induction of auto-reactive $CD4^+$ T cells secondary to the class II presentation of the common SVN sequence (53-67) rather than the reported uncommon 13–27 region.

Generally, the presence of Tregs and regulatory cytokines such as IL-10 usually suppresses the function of self-reactive $CD4^+$ T effectors, so an autoimmune response cannot be detected (Danke et al. 2004; Quezada et al. 2010). In tumor-bearing mice, polyI:C releases the restriction of T cell autoreactivity by Tregs to enhance $CD4^+$ T function in a tumor microenvironment. Although the level of Treg cells increases in MALP2s-stimulated tumor-bearing mice (Yamazaki et al. 2011), the amount of Treg cells is not affected by polyI:C injection (Chua et al. 2014). Signs of autoimmune diseases have not yet been observed in mice that received intermittent administration of polyI:C under our conditions. Further studies on the function of regulatory factors in tumor-bearing mice after treatment with various adjuvants are needed to determine the balance between $CD4^+$ T effector functions and regulatory factors including Tregs (Quezada et al. 2010; Corthay et al. 2005).

It has been reported that treatment of murine glioma with DCs loading MmSVN long overlapping peptide covering CD4 and CD8 epitopes (DC therapy) conferred good prognosis on tumor-bearing mice (Ciesielski et al., 2008). In previous trials on peptide vaccine therapy, SVN2B peptide + IFN-α resulted in clinical improvements and enhanced immunological responses of patients (Kameshima et al. 2013). Treatment with SVN2B peptide alone did not result in good prognosis or effective tumor regression in late stage patients with cancer, however (Tsuruma et al. 2008; Honma et al. 2009). These results suggest that both killer and helper T cells are required for *in vivo* induction of tumor regression, as previously suggested (Perez-Diez et al. 2007). NK cells, Mfs, and soluble and angiogenetic factors might be involved in tumor rejection (Shime et al. 2012; Müller-Hermelink et al., 2008; Coussens and Werb 2002) in addition to Ag + polyI:C. According to the study with Ag and polyI:C, a protein or long peptide Ag containing CD4 epitopes, adjuvant RNA and additional factors that disable immunoregulatory factors, are required to effectively induce TAA-specific killer and helper T cell proliferation and subsequent tumoricidal activity in future studies (Casares et al. 2001). Ag peptides should be designed to present both class I and class II peptides on DCs to facilitate proliferation of $CD4^+$ T cells and Ab production. Methods for inducing potential $CD8^+$ CTLs against tumors still need to be considered.

Competing interests

The authors have declared that no competing interest exists.

Acknowledgements

We are grateful to members in our laboratories. JK is a Research Fellow of the Japan Society for the Promotion of Science. This work was supported in part by Grants-in-Aid from the Ministry of Education, Science, and Culture and the Ministry of Health, Labor, and Welfare of Japan, and by a MEXT Grant-in-Project 'the Carcinogenic Spiral', 'the National Cancer Center Research and Development Fund (23-A-44)'. Financial support by the Takeda Science Foundation, the Yasuda Cancer Research Foundation and the Ono Foundation are gratefully acknowledged.

Appendix A. Supplementary data

Supplementary data associated with this article can be found, in the online version, at http://dx.doi.org/10.1016/j.imbio.2014.08.017.

References

Ahonen, C.L., Doxsee, C.L., McGurran, S.M., Riter, T.R., Wade, W.F., Barth, R.J., Vasilakos, J.P., Noelle, R.J., Kedl, R.M., 2004. Combined TLR and CD40 triggering induces potent CD8+ T cell expansion with variable dependence on type I IFN. J. Exp. Med. 199, 775–784.

Altieri, D.C., 2001. The molecular basis and potential role of survivin in cancer diagnosis and therapy. Trends Mol. Med. 7, 542–547.

Akazawa, T., Ebihara, T., Okuno, M., Okuda, Y., Shingai, M., Tsujimura, K., Takahashi, T., Ikawa, M., Okabe, M., Inoue, N., Okamoto-Tanaka, M., Ishizaki, H., Miyoshi, J., Matsumoto, M., Seya, T., 2007. Antitumor NK activation induced by the Toll-like receptor 3-TICAM-1 (TRIF) pathway in myeloid dendritic cells. Proc. Natl. Acad. Sci. U. S. A. 104, 252–257.

Ambrosini, G., Adida, C., Altieri, D.C., 1997. A novel anti-apoptosis gene, survivin, expressed in cancer and lymphoma. Nat. Med. 3, 917–921.

Andersen, M.H., Pedersen, L.O., Becker, J.C., Straten, P.T., 2001. Identification of a cytotoxic T lymphocyte response to the apoptosis inhibitor protein survivin in cancer patients. Cancer Res. 61, 869–872.

Azuma, M., Ebihara, T., Oshiumi, H., Matsumoto, M., Seya, T., 2012. Cross-priming for antitumor CTL induced by soluble Ag + polyI:C depends on the TICAM-1 pathway in mouse CD11c(+)/CD8α(+) dendritic cells. Oncoimmunology 1, 581–592.

Azuma, M., Matsumoto, M., Seya, T., 2013. PolyI:C-derived dendritic cell maturation and cellular effectors depend on TICAM-1-Batf3 axis in mice. Proc. Jpn. Cancer Assoc. 72, 126.

Bevan, M.J., 1976. Cross-priming for a secondary cytotoxic response to minor H antigens with H-2 congenic cells which do not cross-react in the cytotoxic assay. J. Exp. Med. 143, 1283–1288.

Casares, N., Lasarte, J.J., de Cerio, A.L., Sarobe, P., Ruiz, M., Melero, I., Prieto, J., Borrás-Cuesta, F., 2001. Immunization with a tumor-associated CTL epitope plus a tumor-related or unrelated Th1 helper peptide elicits protective CTL immunity. Eur. J. Immunol. 31, 1780–1789.

Charalambous, A., Oks, M., Nchinda, G., Yamazaki, S., Steinman, R.M., 2006. Dendritic cell targeting of survivin protein in a xenogeneic form elicits strong CD4+ T cell immunity to mouse survivin. J. Immunol. 177, 8410–8421, 44.

Chua, B.Y., Olson, M.R., Bedoui, S., Sekiya, T., Wong, C.Y., Turner, S.J., Jackson, D.C., 2014. The use of a TLR2 agonist-based adjuvant for enhancing effector and memory CD8 T-cell responses. Immunol. Cell Biol., http://dx.doi.org/10.1038/icb.2013.102.

Ciesielski, M.J., Kozbor, D., Castanaro, C.A., Barone, T.A., Fenstermaker, R.A., 2008. Therapeutic effect of a T helper cell supported CTL response induced by a survivin peptide vaccine against murine cerebral glioma. Cancer Immunol. Immunother. 57, 1827–1835.

Corthay, A., Skovseth, D.K., Lundin, K.U., Rosjo, E., Omholt, H., Hofgaad, P.O., Haraldsen, G., Bogen, B., 2005. Primary antitumor immune response mediated by CD4+ T cells. Immunity 22, 371–383.
Coussens, L.M., Werb, Z., 2002. Inflammation and cancer. Nature 420, 860–867.
Danke, N.A., Koelle, D.M., Yee, C., Beheray, S., Kwok, W.W., 2004. Autoreactive T cells in healthy individuals. J. Immunol. 172, 5967–6572.
Fukuda, S., Pelus, L.M., 2006. Survivin, a cancer target with an emerging role in normal adult tissues. Mol. Cancer Ther. 5, 1087–1098.
Gebe, J.A., Falk, B.A., Rock, K.A., Kochik, S.A., Heninger, A.K., Reijonen, H., Kwok, W.W., Nepom, G.T., 2003. Low-avidity recognition by CD4+ T cells directed to self-antigens. Eur. J. Immunol. 33, 1409–1417.
Gotoh, M., Takasu, H., Harada, K., Yamaoka, T., 2002. Development of HLA-A2402/K^b transgenic mice. Int. J. Cancer 100, 565–570.
Hirohashi, Y., Torigoe, T., Maeda, A., Nabeta, Y., Kamiguchi, K., Sato, T., Yoda, J., Ikeda, H., Hirata, K., Yamanaka, N., Sato, N., 2002. An HLA-A24-restricted cytotoxic T lymphocyte epitope of a tumor-associated protein, survivin. Clin. Cancer Res. 8, 1731–1739.
Honma, I., Kitamura, H., Torigoe, T., Takahashi, A., Tanaka, T., Sato, E., Hirohashi, Y., Masumori, N., Tsukamoto, T., Sato, N., 2009. Phase I clinical study of anti-apoptosis protein survivin-derived peptide vaccination for patients with advanced or recurrent urothelial cancer. Cancer Immunol. Immunother. 58, 1801–1807.
Idenoue, S., Hirohashi, Y., Torigoe, T., Sato, Y., Tamura, Y., Hariu, H., Yamamoto, M., Kurotaki, T., Tsuruma, T., Asanuma, H., Kanaseki, T., Ikeda, H., Kashiwagi, K., Okazaki, M., Sasaki, K., Sato, T., Ohmura, T., Hata, F., Yamaguchi, K., Hirata, K., Sato, N., 2005. A potent immunogenic general cancer vaccine that targets survivin, an inhibitor of apoptosis proteins. Clin. Cancer Res. 11, 1474–1482.
Janssen, E.M., Lemmens, E.E., Wolfe, T., Christen, U., von Herrath, M.G., et al., 2003. CD4+ T cells are required for secondary expansion and memory in CD8+ T lymphocytes. Nature 421, 852–856.
Kameshima, H., Tsuruma, T., Kutomi, G., Shima, H., Iwayama, Y., Kimura, Y., Imamura, M., Torigoe, T., Takahashi, A., Hirohashi, Y., Tamura, Y., Tsukahara, T., Kanaseki, T., Sato, N., Hirata, K., 2013. Immunotherapeutic benefit of α-interferon (IFNα) in survivin2B-derived peptide vaccination for advanced pancreatic cancer patients. Cancer Sci. 104, 124–129.
Kobayashi, K., Hatano, M., Otaki, M., Ogasawara, T., Tokuhisa, T., 1999. Expression of a murine homologue of the inhibitor of apoptosis protein is related to cell proliferation. Proc. Natl. Acad. Sci. U. S. A. 96, 1457–1462.
Lee, M.K.4th, Xu, S., Fitzpatrick, E.H., Sharma, A., Graves, H.L., Czerniecki, B.J., 2013. Inhibition of CD4+CD25+ regulatory T cell function and conversion into Th1-like effectors by a Toll-like receptor-activated dendritic cell vaccine. PLOS ONE 8, e74698.
Li, F., 2005. Role of survivin and its splice variants in tumorigenesis. Br. J. Cancer 92, 212–216.
Mahotka, C., Wenzel, M., Springer, E., Gabbert, H.E., Gerharz, C.D., 1999. Survivin-deltaEx3 and survivin-2B: two novel splice variants of the apoptosis inhibitor survivin with different antiapoptotic properties. Cancer Res. 59, 6097–6102.
Mahotka, C., Liebmann, J., Wenzel, M., Suschek, C.V., Schmitt, M., Gabbert, H.E., Gerharz, C.D., 2002. Differential subcellular localization of functionally divergent surviving splice variants. Cell Death Differ. 9, 1334–1342.
Mak, T.W., Shahinian, A., Yoshinaga, S.K., Wakeham, A., Boucher, L.M., Pintilie, M., Duncan, G., Gajewska, B.U., Gronski, M., Eriksson, U., Odermatt, B., Ho, A., Bouchard, D., Whorisky, J.S., Jordana, M., Ohashi, P.S., Pawson, T., Bladt, F., Tafuri, A., 2003. Costimulation through the inducible costimulator ligand is essential for both T helper and B cell functions in T cell-dependent B cell responses. Nat. Immunol. 4, 765–772.
Matsumoto, M., Seya, T., 2008. TLR3: interferon induction by double-stranded RNA including poly(I:C). Adv. Drug Deliv. Rev. 60, 805–812.
Mills, K.H., 2011. TLR-dependent T cell activation in autoimmunity. Nat. Rev. Immunol. 11, 807–822.
Müller-Hermelink, N., Braumüller, H., Pichler, B., Wieder, T., Mailhammer, R., Schaak, K., Ghoreschi, K., Yazdi, A., Haubner, R., Sander, C.A., Mocikat, R., Schwaiger, M., Förster, I., Huss, R., Weber, W.A., Kneilling, M., Röcken, M., 2008. TNFR1 signaling and IFN-gamma signaling determine whether T cells induce tumor dormancy or promote multistage carcinogenesis. Cancer Cell 13, 507–518.
Nishiguchi, M., Matsumoto, M., Takao, T., Hoshino, M., Shimonishi, Y., Tsuji, S., Begum, N.A., Takeuchi, O., Akira, S., Toyoshima, K., Seya, T., 2001. Mycoplasma *fermentans* lipoprotein M161Ag-induced cell activation is mediated by Toll-like receptor 2: role of N-terminal hydrophobic portion in its multiple functions. J. Immunol. 166, 2610–2616.
Okada, H., Bakal, C., Shahinian, A., Elia, A., Wakeham, A., Suh, W.K., Duncan, G.S., Ciofani, M., Rottapel, R., Zuniga-Pflucker, J.C., Mak, T.W., 2004. Survivin loss in thymocytes triggers p53-mediated growth arrest and p53-independent cell death. J. Exp. Med. 199, 399–410.
Osen, W., Soltek, S., Song, M., Leuchs, B., Steitz, J., Tüting, T., Eichmüller, S.B., Nguyen, X.D., Schadendorf, D., Paschen, A., 2010. Screening of human tumor antigens for CD4 T cell epitopes by combination of HLA-transgenic mice, recombinant adenovirus and antigen peptide libraries. PLOS ONE 5, e14137.
Perez-Diez, A., Joncker, N.T., Choi, K., Chan, W.F., Anderson, C.C., Lantz, O., Matzinger, P., 2007. CD4 cells can be more efficient at tumor rejection than CD8 cells. Blood 109, 5346–5354.
Quezada, S.A., Simpson, T.R., Peggs, K.S., Merghoub, T., Vider, J., Fan, X., Blasberg, R., Yagita, H., Muranski, P., Antony, P.A., Restifo, N.P., Allison, J.P., 2010. Tumor-reactive CD4(+)T cells develop cytotoxic activity and eradicate large established melanoma after transfer into lymphopenic hosts. J. Exp. Med. 207, 637–650.
Ridge, J.P., Di Rosa, F., Matzinger, P., 1998. A conditioned dendritic cell can be a temporal bridge between a CD4+ T-helper and a T-killer cell. Nature 393, 474–478.
Rosenberg, S.A., Yang, J.C., Restifo, N.P., 2004. Cancer immunotherapy: moving beyond current vaccines. Nat. Med. 10, 909–915.
Sawahata, R., Shime, H., Yamazaki, S., Inoue, N., Akazawa, T., Fujimoto, Y., Fukase, K., Matsumoto, M., Seya, T., 2011. Failure of mycoplasma lipoprotein MALP-2 to induce NK cell activation through dendritic cell TLR2. Microbes Infect. 13, 350–358.
Schmitz, M., Diestelkoetter, P., Weigle, B., Schmachtenberg, F., Stevanovic, S., Ockert, D., Rammensee, H.G., Rieber, E.P., 2000. Generation of survivin-specific CD8+ T effector cells by dendritic cells pulsed with protein or selected peptides. Cancer Res. 60, 4845–4849.
Schulz, O., Diebold, S.S., Chen, M., Näslund, T.I., Nolte, M.A., Alexopoulou, L., Azuma, Y.T., Flavell, R.A., Liljeström, P., Reis e Sousa, C., 2005. Toll-like receptor 3 promotes cross-priming to virus-infected cells. Nature 433, 887–892.
Seya, T., Matsumoto, M., 2009. The extrinsic RNA-sensing pathway for adjuvant immunotherapy of cancer. Cancer Immunol. Immunother. 58, 1175–1184.
Seya, T., Azuma, M., Matsumoto, M., 2013. Targeting TLR3 with no RIG-I/MDA5 activation is effective in immunotherapy for cancer. Expert Opin. Ther. Targets 17, 533–544.
Shime, H., Matsumoto, M., Oshiumi, H., Tanaka, S., Nakane, A., Iwakura, Y., Tahara, H., Inoue, N., Seya, T., 2012. Toll-like receptor 3 signaling converts tumor-supporting myeloid cells to tumoricidal effectors. Proc. Natl. Acad. Sci. U. S. A. 109, 2066–2071.
Topalian, S.L., Gonzales, M.I., Parkhurst, M., Li, Y.F., Southwood, S., Sette, A., Rosenberg, S.A., Robbins, P.F., 1996. Melanoma-specific CD4+ T cells recognize nonmutated HLA-DR-restricted tyrosinase epitopes. J. Exp. Med. 183, 1965–1971.
Tsuruma, T., Iwayama, Y., Ohmura, T., Katsuramaki, T., Hata, F., Furuhata, T., Yamaguchi, K., Kimura, Y., Torigoe, T., Toyota, N., Yagihashi, A., Hirohashi, Y., Asanuma, H., Shimozawa, K., Okazaki, M., Mizushima, Y., Nomura, N., Sato, N., Hirata, K., 2008. Clinical and immunological evaluation of anti-apoptosis protein, survivin-derived peptide vaccine in phase I clinical study for patients with advanced or recurrent breast cancer. J. Transl. Med. 6, 24.
Yamazaki, S., Okada, K., Maruyama, A., Matsumoto, M., Yagita, H., Seya, T., 2011. TLR2-dependent induction of IL-10 and Foxp3+ CD25+ CD4+ regulatory T cells prevents effective anti-tumor immunity induced by Pam2 lipopeptides in vivo. PLOS ONE 6, e18833.

nature COMMUNICATIONS

ARTICLE

Received 7 Nov 2014 | Accepted 13 Jan 2015 | Published 18 Feb 2015

DOI: 10.1038/ncomms7280

Defined TLR3-specific adjuvant that induces NK and CTL activation without significant cytokine production *in vivo*

Misako Matsumoto[1], Megumi Tatematsu[1], Fumiko Nishikawa[1], Masahiro Azuma[1,†], Noriko Ishii[1], Akiko Morii-Sakai[1], Hiroaki Shime[1] & Tsukasa Seya[1]

Ligand stimulation of the Toll-like receptors (TLRs) triggers innate immune response, cytokine production and cellular immune activation in dendritic cells. However, most TLR ligands are microbial constituents, which cause inflammation and toxicity. Toxic response could be reduced for secure immunotherapy through the use of chemically synthesized ligands with defined functions. Here we create an RNA ligand for TLR3 with no ability to activate the RIG-I/MDA5 pathway. This TLR3 ligand is a chimeric molecule consisting of phosphorothioate ODN-guided dsRNA (sODN-dsRNA), which elicits far less cytokine production than poly(I:C) *in vitro* and *in vivo*. The activation of TLR3/TICAM-1 pathway by sODN-dsRNA effectively induces natural killer and cytotoxic T cells in tumour-loaded mice, thereby establishing antitumour immunity. Systemic cytokinemia does not occur following subcutaneous or even intraperitoneal administration of sODN-dsRNA, indicating that TICAM-1 signalling with minute local cytokines sufficiently activate dendritic cells to prime tumoricidal effectors *in vivo*.

[1] Department of Microbiology and Immunology, Hokkaido University Graduate School of Medicine, Kita 15, Nishi 7, Kita-ku, Sapporo 060-8638, Japan. † Present address: Department of Pathology and Cellular Biology, University of Montreal, 2900 Edouard-Montpetit, Montreal, Quebec, Canada H3T 1J4. Correspondence and requests for materials should be addressed to M.M. (email: matumoto@pop.med.hokudai.ac.jp) or to T.S. (email: seya-tu@pop.med.hokudai.ac.jp).

Double-stranded (ds) RNA is often a signature of viral infection, which induces production of type I interferon (IFN) and inflammatory cytokines[1,2]. Its putative analogue polyinosinic:polycytidylic acid (poly(I:C)) exhibits both strong antiviral and anticancer potential[3,4]. Poly(I:C) has been considered a promising adjuvant for cancer immunotherapy for several decades[4–6]. In mouse models, growth retardation of syngenic implant tumours is observed following administration of poly(I:C)[7,8], which is due to dendritic cell (DC)-derived natural killer (NK) and cytotoxic T-cell (CTL) activity[9,10]. Nevertheless, it has not been successfully used therapeutically in patients with cancer[5,6]. The amount of poly(I:C) required for an adequate therapeutic response causes side effects, including arthlargia, fever, erythema and sometimes life-threatening endotoxin-like shock[5,6], which have prevented application of this dsRNA analogue from the clinical use. These side effects may be related to cytokine storm induced by dsRNA, although the situation is somewhat alleviated when minimal poly(I:C)-LC (poly-L-lysine and methylcellulose) is used instead of effector-inducible doses of mere poly(I:C) alone[5,6,11].

According to recent understanding on pattern recognition of innate immunity, poly(I:C) is a ligand for multiple pattern recognition receptors (PRRs), including protein kinase R, retinoic acid-inducible gene-I (RIG-I), melanoma differentiation-associated gene 5 (MDA5) and Toll-like receptor (TLR) 3 (refs 1,4,12). Virus replication usually produces dsRNA within the cytoplasm of infected cells and stimulates the cytoplasmic RNA sensors[12,13]. In contrast, TLR3 is activated when dsRNA liberated from virus-infected cells is internalized into the endosome of non-infected phagocytes[4,14], such as DCs and macrophages. Type I IFN and DC-mediated immune responses are evoked to suppress virus replication. Physiologically, these responses occur in a complex manner, therefore, what happens *in vivo* when only a single receptor is stimulated remains to be elucidated, whereas what happens *in vivo* when a single gene is disrupted has been reported in knockout (KO) mouse studies[1]. It is therefore crucial in drug design to create PRR ligands specific for each PRR for the development of immune adjuvant.

Regression of tumour with a lesser major histocompatibility complex expression[15] is caused by reciprocal activation of NK cells by poly(I:C)-stimulated DC[9,16]. However, in antitumour immunity, constitutive proliferation of antitumour CTL is important and antigen (Ag)-presenting DC must capture not only innate patterns but also tumour-associated Ag (TAA) for their cross-priming[10,17]. CD8α^+ DC in mouse lymphoid tissue[10,18,19] and CD103$^+$ and CD141$^+$ DCs in humans[18–20] are representative subsets that express TLR3 and induce efficient Ag cross-presentation in response to dsRNA enabling presentation of Ags to CD8$^+$ T cells on their major histocompatibility complex class I proteins. In contrast, interleukin (IL)-12, IL-6, tumour necrosis factor (TNF)-α and IFN-α/β are the main mediators released in the serum secondary to exogenously administered poly(I:C)[4,20,21]. Studies in KO mice suggested that TLR3 has a pivotal role in inducing cross-presentation[10,17], but its role is marginal in systemic cytokine/IFN production *in vivo*[21]. Most cytokines (except IL-12 p40) and type I IFN detected in serum are attributable to poly(I:C)'s stimulation of RIG-I and/or MDA5, that is, the mitochondrial antiviral-signalling protein (MAVS) pathway[12,21]. CTL/NK cell activation and robust cytokine production can be assigned, although partly overlapping, to the TLR3/Toll-IL-1 receptor domain-containing adaptor molecule (TICAM)-1 or MAVS pathway, respectively.

Here we generated synthetic dsRNA derivatives expected to specifically act on TLR3, but not on RIG-I/MDA5. These ligands exhibited strong activity in inducing antitumour CTL and NK cells and caused marked regression of tumours without off-target effects including significant increases of serum cytokine/IFN levels in mouse models.

Results

Design of novel TLR3 agonist. What we experienced in developing an RNA adjuvant was that: very little *in vitro* transcribed dsRNAs entered the human cells[22], whereas poly(I:C) as well as CpG or control GpC phosphorothioate oligodeoxynucleotides (sODNs) reached the endosome in human myeloid DCs and epithelial cells. Poly(I:C) and sODNs appeared to share the uptake receptor[23]. To deliver dsRNA to endosome TLR3, we have connected sODN to 5′ sense RNA and annealed it with antisense RNA (Fig. 1a) to guide dsRNA internalization into TLR3-positive endosomes. The RNA source was chosen from a vaccine strain of measles virus (MV), as children around the world undergo MV vaccination without severe adverse events. Because >40 bp dsRNA may be the minimal length for activation of TLR3 (ref. 24), we selected the region of defective interference RNA in the vaccine MV that causes no RNA interference[25].

Because direct chemical synthesis of long sequences of RNA was unfeasible in our laboratory until recently, we first made the RNA duplex structures by *in vitro* transcription and annealing. sODN was connected via a linker DNA to dsRNA, so the three-chain structures were first designed (Fig. 1b) to carry forward by many trial-and-error tests for a specific TLR3 agonist. A GpC-type sODN cap cM362 (Fig. 1a,b) facilitates targeting to TLR3-positive endosomes, does not activate TLR9 and blocks dsRNA-mediated RIG-I/MDA5 activation; therefore it meets our criteria for a single PRR agonist.

Testing function of *in vitro* transcribed sODN-dsRNAs. Various kinds of sODN-dsRNA hybrid molecules were prepared by *in vitro* transcription and annealing (Supplementary Fig. 1a, Supplementary Tables 1 and 2). In preliminary experiments to screen for a preferential sODN-dsRNA, we tested reporter gene (Luc125 for IFN-β promoter) activation in HEK293 cells expressing human TLR3.

sODN-dsRNAs with dsRNA of >99 bp in length induced TLR3-dependent IFN-β-promoter activation similar to that induced by poly(I:C) in the presence or absence of fetal calf serum (FCS), whereas sODN-dsRNAs with dsRNA of <79 bp induced hardly any activation of TLR3 (Supplementary Fig. 1b,c). Notably, none of the sODN-dsRNAs examined were able to activate cytoplasmic RNA sensors when transfected into HEK293 cells (Supplementary Fig. 2). We examined whether GpC motif or the length of sODN influenced the uptake of sODN-dsRNA. TLR3-mediated IFN-β promoter activation by sODN-dsRNA was independent of the presence of a GpC motif of sODN but dependent on the length; almost >20-mer of sODN is required for full activation of endosomal TLR3 (Supplementary Fig. 3). 139 bp dsRNA and control B-type (c2006) or C-type (cM362) sODN were good candidates for activation of endosomal TLR3 with no TLR9 activation.

We next examined the internalization of Cy3-labelled cM362-dsRNA (cM362-79, cM362-99 and cM362-139) in HeLa cells. cM362-dsRNAs were all similarly bound to the cell surface at 4 °C, but dsRNA73 and dsRNA139 without cM362 could not bind (Supplementary Fig. 4). When cells were incubated at 37 °C, cM362-99 and cM362-139 both entered the cells more quickly than cM362 and cM362-79, localized in the early endosome after 15 min incubation and were retained for up to 120 min, whereas cM362 and cM362-79 co-localized with EEA1 at a later time point (30 min) and quickly moved to the lysosomes. Localization of cM362-139 in the lysosomes was observed after 60 min

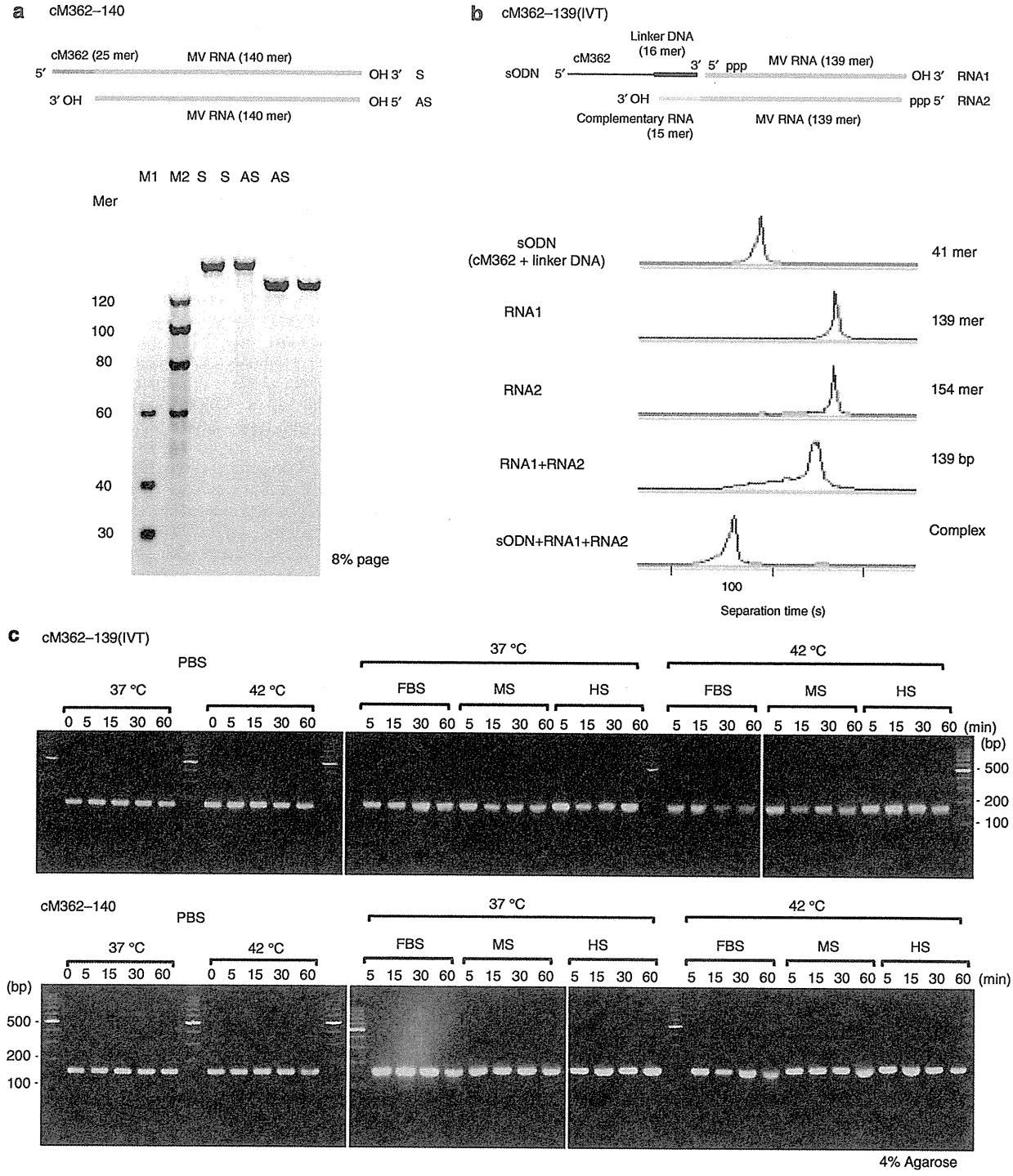

Figure 1 | Preparation of cM362-139 and cM362-140. (**a**) Schematic diagram of cM362-140. cM362-140 consists of chemically synthesized two nucleotide strands. The sense strand (S) is a 140 mer RNA capped with cM362 (25 mer) at 5′ site. The antisense strand (AS) is the complementary 140 mer RNA. Five pmol of S and AS RNAs were analysed on 8% PAGE containing 7M urea. M1 and M2, RNA size markers. (**b**) Schematic diagram of cM362-139(IVT) and its electropherograms. cM362-139(IVT) consists of three nucleotide strands, sODN (cM362 + linker DNA; 41 mer), *in vitro* transcribed sense RNA strand (RNA1; 139 mer) and antisense RNA strand (RNA2; 154 mer). All sequences of DNA and RNAs are described in Supplementary Tables. sODN, RNA1, RNA2, dsRNA (RNA1 + RNA2) and complex cM362-139 (sODN + RNA1 + RNA2) were analysed using multi-channel microchip electrophoresis. (**c**) Stability of cM362-139(IVT) and cM362-140. cM362-139(IVT) and cM362-140 were incubated in PBS with or without 10% heat-inactivated FBS, mouse serum (MS) or human serum (HS) at 37 °C or 42 °C for indicated time points. Aliquots containing 0.1 μg of treated cM362-dsRNAs were loaded onto a 4% agarose gel.

incubation, which was relatively slow compared with cM362-99 (Supplementary Fig. 4). These results suggested that the length of dsRNA together with the presence of cM362 influences the internalization speed and retention time in the TLR3-situated early endosome.

The abilities of cM362-dsRNAs to induce cytokine production were then examined using splenic DCs from wild-type and TLR3-deficient mice. cM362-79 and -139 induced a slight increase in TNF-α and IL-6 production by splenic CD11c$^+$ DCs in a TLR3-dependent manner (Supplementary Fig. 5a). Again, cM362-dsRNAs did not activate cytoplasmic RNA sensors in mouse splenic CD11c$^+$ DCs (Supplementary Fig. 5b). Thus, the chimeric compound cM362-139 appears to possess novel features that enable it to be quickly delivered to TLR3-positive endosomes, retained for a long period in the endosomes, and activate TLR3 but not RIG-like receptor (RLR).

As a TLR3-specific agonist with high activity, we selected cM362-139 for further *in vivo* studies with tumour-loaded mice.

Chemical synthesis of cM362-140. As chemical synthesis of sODN-dsRNA is indispensable for complying with good manufacturing practice (GMP) criteria, we started trials for chemical synthesis of cM362-140 (Fig. 1a), and its activity was analysed in comparison with *in vitro* transcribed cM362-139 (Fig. 1a,b). A synthesized 165 mer sense cM362-RNA hybrid and a 140mer antisense RNA, both of which consisted of single bands on 8% polyacrylamide gel electrophoresis (PAGE) and high-performance liquid chromatography/mass spectrometry analysis were annealed to make cM362-140 (Fig. 1a, lower panel). First, the degradability of cM362-139(IVT) and chemically synthesized cM362-140 were tested under different conditions. Both compounds were stable during incubation in PBS with or without 10% FBS, mouse serum or human serum at 37 °C for 60 min. cM362-139(IVT) was slightly degraded in PBS containing FBS or mouse serum but not human serum during incubation at 42 °C (Fig. 1c). Notably, cM362-139(IVT) was susceptible to degradation by nucleases during incubation in RNase-free water containing 10% FBS or mouse serum, but relatively resistant to human serum (Supplementary Fig. 6). In contrast, cM362-140 was quite stable under all these conditions. Thus, synthetic cM362-140 consisting of the cM362-capped RNA strand and antisense RNA strand was found to be more resistant to serum nucleases than cM362-139(IVT) consisting of three nucleotide strands.

cM362-140 activates TLR3 but not cytoplasmic RNA sensors. cM362-140 efficiently induced TLR3-dependent IFN-β promoter activation similar to cM362-139(IVT), when it was used to stimulate HEK293 cells expressing human TLR3 by simple addition or endosomal delivery (Fig. 2a, left and centre panels). Activation of cytoplasmic RNA/DNA sensors by cM362-140 was hardly observed in HEK293 cells similar to cM362-139(IVT) (Fig. 2a, right panel). To address the potential of cM362-140 for cytokine induction, splenic DCs from wild-type, *Tlr3*$^{-/-}$ or *Mavs*$^{-/-}$ mice were stimulated with poly(I:C), cM362-139(IVT), control synthetic dsRNA140 or cM362-140, either alone or complexed with N-(1-(2,3-Dioleoyloxy)propyl)-N, N, N-trimethylammonium methyl-sulfate) (DOTAP) to deliver them to endosomes, or complexed with Lipofectamine to deliver them to cytoplasm. Extracellular addition of cM362-139(IVT) and cM362-140 to splenic DCs induced a subtle increase in TNF-α, IL-6 and IFN-β production compared with poly(I:C) treatment, whereas synthetic dsRNA140 (with no GpC) did not induce any cytokine over the detection limits (Fig. 2b, left panels). Endosomal delivery of cM362-139(IVT) or cM362-140 with DOTAP also induced minimal levels of TNF-α, IL-6 and IFN-β dependent upon TLR3 (Fig. 2b, centre panels). When the compounds were transfected into cytoplasm with Lipofectamine, MAVS-dependent cytokine production was barely observed with cM362-140, whereas only low levels of IL-6 and IFN-β were induced with cM362-139 in TLR3 KO DC (Fig. 2b, right panel). This MAVS activity may reflect the exposure of a few 5′-triphosphated species of cM362-139(IVT) due to minor RNA degradation. These results indicate that cM362-140 targets endosomal TLR3 and activate the TICAM-1 pathway in both human and mouse cells.

***In vivo* cytokine induction by cM362-140.** Injection of poly(I:C) into mouse peritoneal cavity strongly induced proinflammatory cytokine production in a TLR3-independent manner and high level of TNF-α and IL-6 were detected in sera at 3 h after injection (Fig. 3a). In contrast, both cM362-140 and cM362-139(IVT) hardly induced cytokine production and serum TNF-α, IL-6 and IL-10 levels were very low, which is mediated by TLR3 (Fig. 3a). Unlike poly(I:C), cM362-140 or -139(IVT) induced undetectable levels of IFN-β in wild-type mouse sera (Supplementary Fig. 7).

A subcutaneous (s.c.) injection of cM362-140 induced the mRNAs of IFN-β and IL-6, but not TNF-α, in the inguinal and axillary lymph nodes (LNs) and spleen; the expression level was lower than that induced by poly(I:C) (Fig. 3b). These results suggest that TLR3-specific activation with cM362-140 results in low levels of cytokine production *in vivo* either by intraperitoneal (i.p.) or s.c. administration.

EG7 tumour regression by CTL induced by cM362-139/140. The next question was whether cM362-139(IVT) causes tumour growth retardation as observed with poly(I:C). EG7 cells (a lymphoma cell line containing ovalbumin, OVA) were inoculated into the back of wild-type (WT) C57BL/6 mice, and the indicated materials were injected s.c. around the EG7 tumour that developed (Fig. 4). Tumour growth was mildly retarded by treatment with poly(I:C) or cM362-139(IVT) alone (Fig. 4a). Combination therapy of OVA and poly(I:C) or cM362-139(IVT) resulted in complete remission of EG7 tumour > 12 days after the treatment (Fig. 4a). The results infer that the combination of RNA adjuvant + tumour Ag exerts antitumour immune effect in spite of the low induction of proinflammatory cytokines.

We next tested whether s.c. injection of cM362-139(IVT) plus OVA induced CTL proliferation. The OVA tetramer assay and IFN-γ production were employed to evaluate OVA-specific CD8$^+$ T-cell activation. Combination therapy of cM362-139(IVT) with OVA exhibited an increase in the frequency of Ag-specific CD8$^+$ T cells comparable to poly(I:C) with OVA (Fig. 4b). Ag-specific CD8$^+$ T cells clonally proliferated against EG7 as *in vitro* cytotoxicity was directed exclusively to EG7 in mice stimulated with cM362-139(IVT) with OVA (Fig. 4c) as well as poly(I:C) with OVA[9]. EG7 growth retardation by cM362-139(IVT) with OVA was largely abrogated in TLR3 KO mice (Supplementary Fig. 8), suggesting that cM362-139(IVT) acts on host TLR3 *in vivo*. However, mild tumour growth retardation was still observed with cM362-139(IVT) with OVA in TLR3 KO mice (Supplementary Fig. 8), implying minor involvement of EG7 cell TLR3 or other host RNA sensors, such as RLR[26] and DEAD-box helicases[27], in *in vivo* tumour regression. Yet, tumor cell's TLR3 signaling and chemokine induction might affect tumor remission (refs 28–30).

We finally tested whether chemically synthesized cM362-140 harbours the ability to retard EG7 growth in the same model. The synthetic cM362-140 showed ~80% activity for IFN-β reporter activation compared with cM362-139(IVT) and a single

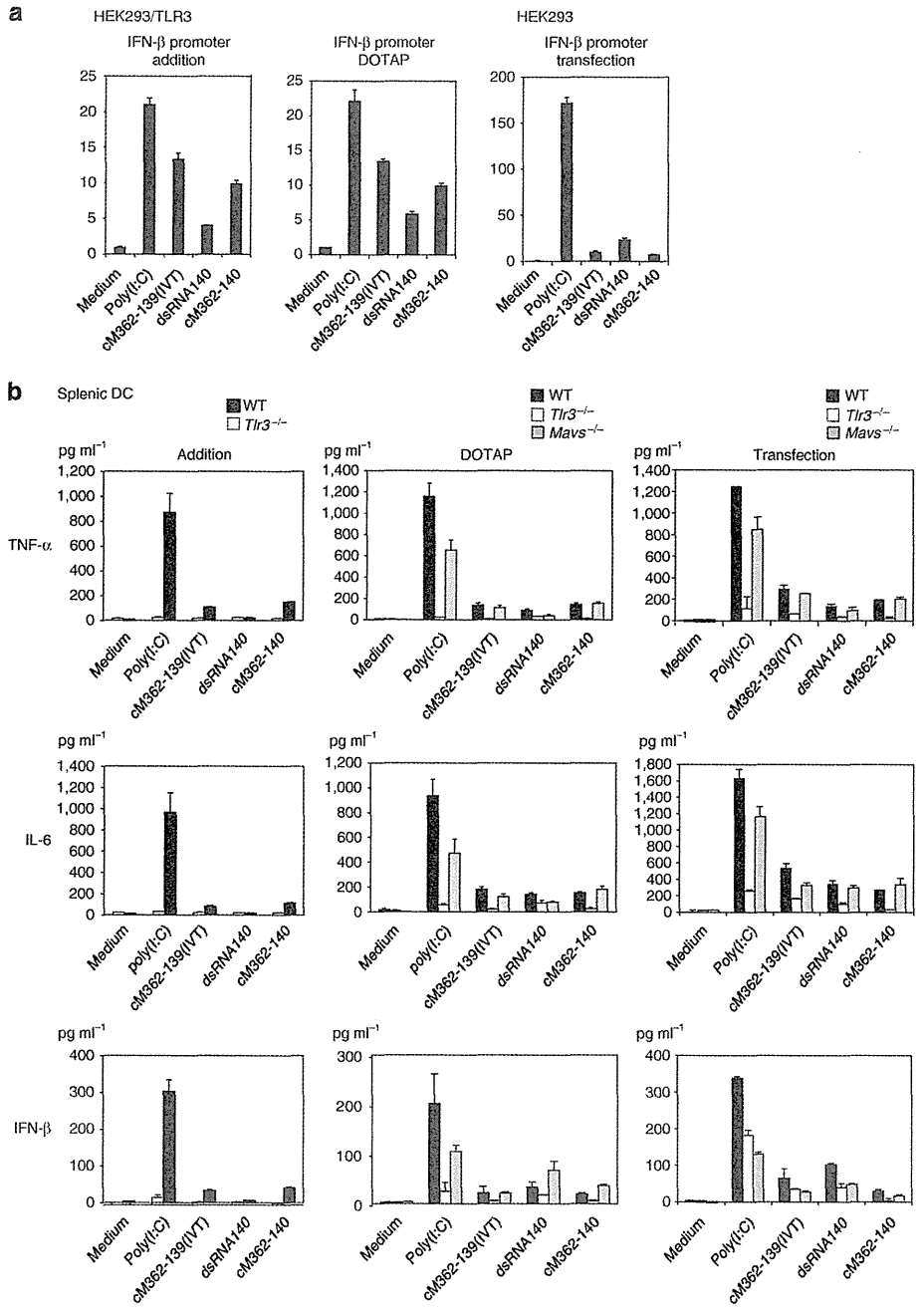

Figure 2 | TLR3-activating ability of cM362-140 in human and mouse cells. (**a**) TLR3-dependent IFN-β promoter activation by cM362-140. HEK293 cells were transiently transfected with IFN-β reporter and phRL-TK together with (left and middle panels) or without the expression plasmid for hTLR3 (right panel). Twenty-four hours after transfection, culture medium was removed and 10 μg ml^{-1} poly(I:C), cM362-139(IVT), dsRNA140 or cM362-140 in fresh medium (left panel), or the same compounds complexed with DOTAP liposomal reagent (middle panel), or with Lipofectamine 2000 (right panel) were added to cells. Luciferase activity was measured 6 h (left and middle panel) or 24 h (right panel) after stimulation, and expressed as fold induction relative to the activity of non-stimulated cells. Representative data from three independent experiments, each performed in triplicate, are shown (mean ± s.d.). (**b**) Splenic CD11c$^+$ DCs (1.0×10^6 per ml) isolated from *Tlr3*$^{-/-}$, *Mavs*$^{-/-}$ or WT mice were stimulated with 10 μg ml^{-1} untreated (left panels), DOTAP liposomal reagent-conjugated (middle panels) or Lipofectamine 2000-conjugated (right panel) nucleic acids as indicated. Twenty-four hours after stimulation, IFN-β in the culture supernatants was quantified using ELISA. TNF-α and IL-6 levels were measured using CBA. Representative data from three to five independent experiments are shown (mean ± s.d.).

treatment with cM362-140 caused barely any regression of EG7 tumours in this model (Fig. 5a). Nevertheless, combination therapy with OVA + cM362-140 still induced tumour growth retardation (Fig. 5a). OVA-specific CD8$^+$ T cells proliferated and activated in the mice stimulated with OVA + cM362-140, as assessed by tetramer assay (Fig. 5b) and IFN-γ production (Fig. 5c). We confirmed that the induction of OVA-specific CD8$^+$ T-cell activation by cM362-140 + OVA largely depends

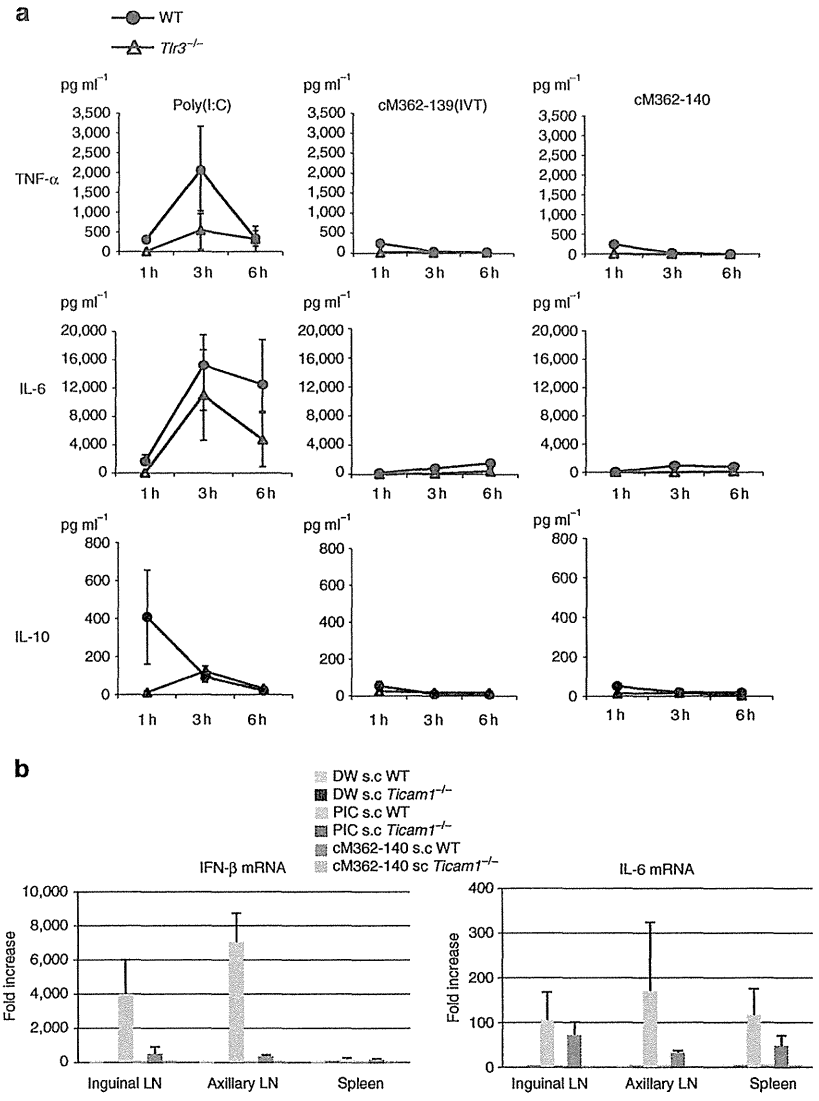

Figure 3 | cM362-139(IVT) and cM362-140 do not induce inflammatory cytokines. (**a**) Wild-type or *Tlr3*$^{-/-}$ female mice (9 week) were injected i.p. with 50 μg poly(I:C), cM362-139(IVT) or cM362-140 in RNase-free water. At timed intervals, blood was collected from the tail vein and TNF-α, IL-6 and IL-10 levels in each sample were measured using a CBA. Data are shown as the mean ± s.e.; $n=3$ mice per group. (**b**) Wild-type or *Ticam*$^{-/-}$ female mice were injected s.c. with distilled water (DW), poly(I:C) or cM362-140 in RNase-free water. After 6 h, spleen, inguinal and axillary LNs were harvested and *IFN-β* and *IL-6* mRNA expressions were quantified by qPCR. Data are expressed as the fold induction relative to the expression in DW-injected mice and shown as the mean ± s.e.; $n=3$ mice per group.

on TLR3/TICAM-1 using KO mice (Supplementary Fig. 9). Although polyI:C induces RIP1/3-mediated necroptosis via TICAM-1 in some tumour lines, cM362-140 was not the case in EG7 tumour (Supplementary Fig. 10). Hence, TLR3 has an important role in inducing cM362-140-mediated immune response and tumour growth retardation in the s.c. setting we employed in this study.

Antigen-specific CD8$^+$ T-cell priming by cM362-139/140. The Ag-specific CD8$^+$ T-cell priming ability of cM362-139/140 in tumour-free settings was next examined using spleen and inguinal LN cells. Wild-type mice were injected s.c. with OVA with or without RNA adjuvants twice per week. Since OVA-specific CD8$^+$ T cells most proliferated in spleen or inguinal LN 4 days after the last injection of OVA + poly(I:C) (Fig. 6a), spleen and LN cells were harvested from mice 4 days after the last adjuvant injection. cM362-139/140 significantly induced OVA-specific CD8$^+$ T-cell proliferation in the inguinal LN and spleen compared with poly(I:C) (Fig. 6b). OVA-specific IFN-γ production in spleen cells was also efficiently induced by cM362-139(IVT) and cM362-140 (Fig. 6c). The TICAM-1 pathway was mainly involved in Ag-specific CD8$^+$ T-cell activation induced by cM362-140 (Fig. 6d).

NK cell-mediated B16 tumour regression by cM362-139/140. Using a C57BL/6-B16 syngeneic NK-sensitive tumour-implant model[9], we evaluated NK-dependent antitumour activity of cM362-139(IVT) injected s.c. around the pre-formed tumour (Fig. 7a). Suppression of tumour growth, determined as reported previously[9], was observed in the group that received cM362-139(IVT) compared with the water-treated group. The retardation of B16 tumour growth appeared to depend on TLR3

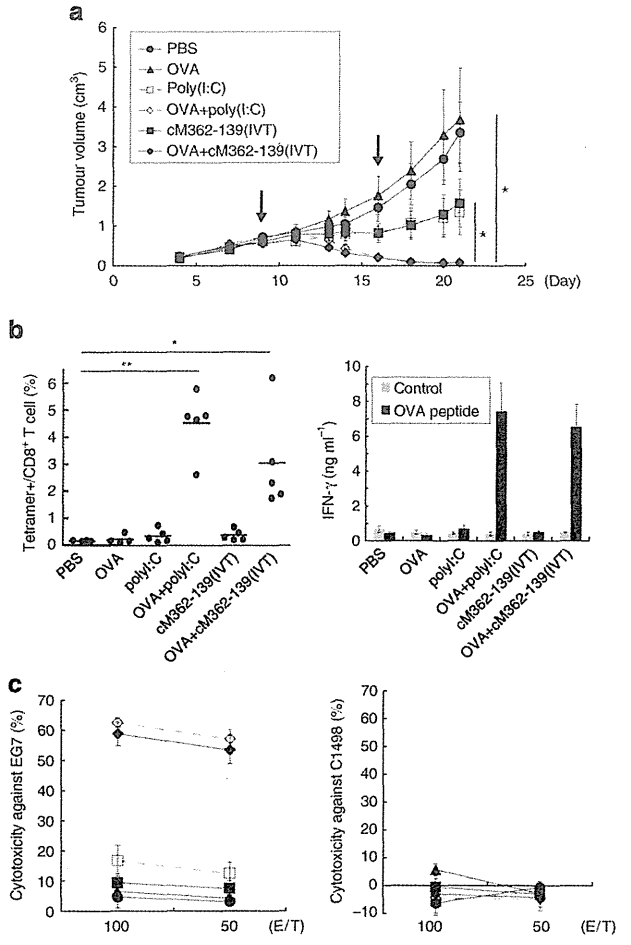

Figure 4 | cM362-139(IVT) induces CTL-mediated tumour regression. (**a**) Antitumour effect of cM362-139(IVT). WT mice were challenged with EG7 cells, and 7 and 14 days later they were s.c. injected with control PBS (●), OVA (▲), polyI:C (□) and OVA + polyI:C (◇) or cM362-139(IVT) (■) or OVA + cM362-139 (◆). Tumour size was evaluated in each group. All error bars used in this figure show ± s.e.m. Data are representative of two independent experiments. Each group consisted of five mice. $^{*}P<0.05$ (ANOVA with Bonferroni's test). (**b**) OVA-specific CTL induction by cM362-139(IVT). Left panel: spleen cells were harvested at day 21 (7 days after 2nd therapy) and the proportion of tetramer-positive cells/CD8$^+$ T cells was evaluated. $^{*}P<0.05$, $^{**}P<0.01$. Right panel: spleen cells were harvested at day 21 as for the left panel. The cells were stimulated with OVA peptide for 3 days and the level of IFN-γ in the culture supernatant was measured. (**c**) Ag-specific cytotoxicity induced by cM362-139(IVT). Splenocytes collected from tumour-bearing mice at day 21 were cultured in the presence of immorbilized EG7 for 5 days. Then, the cytotoxicity against EG7 (left panel) or C1498 (control, right panel) was measured by ^{51}Cr release assay.

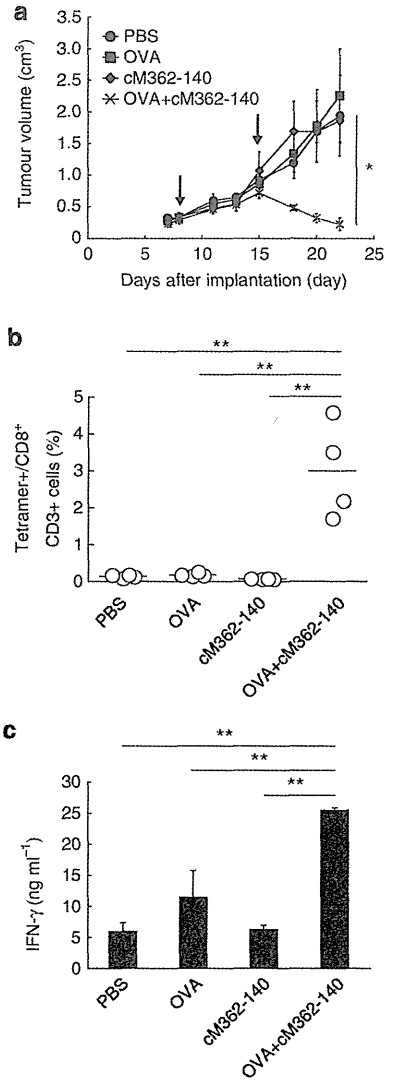

Figure 5 | cM362-140 induces EG7 tumour growth retardation. (**a**) Antitumour effect of cM362-140. As in Fig. 4, tumour-bearing mice were s.c. injected with PBS, OVA, cM362-140 and OVA + cM362-140 at timed intervals (days 8 and 15). Tumour size was evaluated in each group. (**b**) OVA-specific CTL induction by cM362-140. The proportion of tetramer-positive cells/CD8$^+$ T cells in spleen was evaluated at day 22 (7 days after 2nd therapy). (**c**) Ag-specific IFN-γ production induced by cM362-140. Splenocytes were harvested at day 22 and incubated with OVA peptides for 3 days. The level of IFN-γ in the supernatant was measured by ELISA. $^{*}P<0.05$, $^{**}P<0.01$ (ANOVA with Bonferroni's test).

and TICAM-1 (Fig. 7a,b). NK1.1$^+$ cells were involved in this tumour growth retardation (Fig. 7c), consistent with the NK-sensitive properties of B16 cells. No direct tumour cytolysis by macrophages[31] was associated with B16 growth retardation in the cM362-139(IVT) therapy. Splenocytes from the cM362-139(IVT)-treated group exerted higher cytotoxicity than those from the control group *in vitro* (Fig. 7d).

The chemically synthesized TLR3 ligand cM362-140 expressed a similar tumour-suppressing activity against B16 implant melanoma in the same model (Fig. 7e). This cM362-140-mediated NK-tumoricidal activity on B16 tumours was abrogated in *Ticam1*$^{-/-}$ mice (Fig. 7e). Thus, cM362-140 suppresses NK-sensitive tumours *in vivo* via TLR3 by acting as an NK-inducing adjuvant.

Discussion

Cancer immunotherapy relies on suitable adjuvants. Many TAA peptides have been synthesized, but the lack of an appropriate adjuvant to induce an immune response against the peptides has hampered progress in peptide vaccine therapy. Although many candidates, most of which were retrospectively recognized as TLR

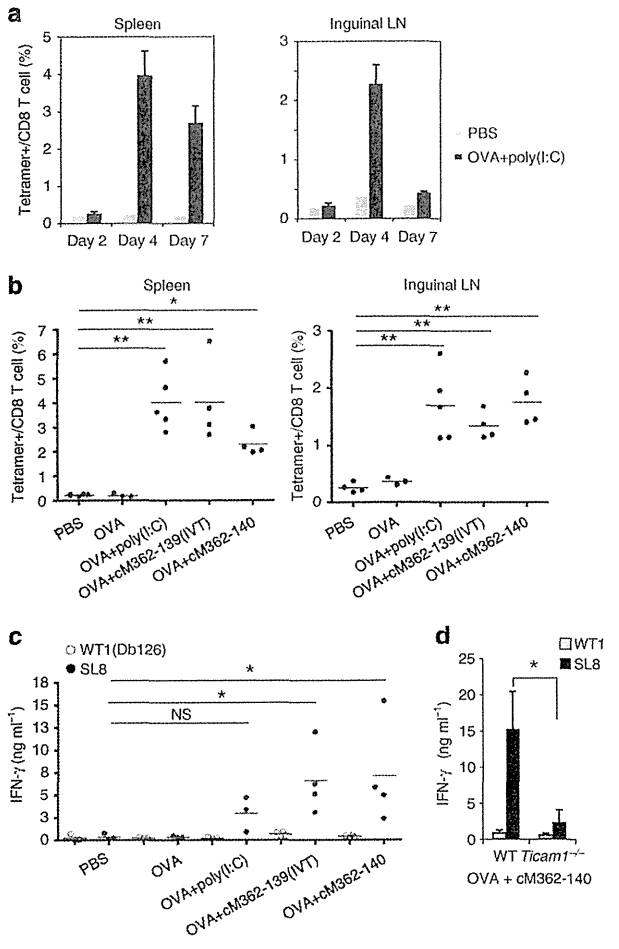

Figure 6 | cM362-139/140-induced antigen-specific CD8 T-cell activation in tumour-free settings. (**a**) Time-course experiments of poly(I:C)-induced antigen-specific CD8 T-cell activation in spleen and inguinal LN. WT mice were injected s.c. with 100 μl PBS or 50 μg poly(I:C) + 100 ng OVA twice per week. Spleen and inguinal LN cells were harvested at 2, 4 or 7 days after the last adjuvant injection and an increase of OVA-specific CD8 T-cell proliferation was evaluated with tetramer assay. (**b**,**c**) WT mice were injected s.c. with PBS, OVA, OVA + 50 μg poly(I:C), OVA + 50 μg cM362-139(IVT) or OVA + 70 μg cM362-140 twice per week. Spleen and inguinal LN cells were harvested 4 days after the last adjuvant injection and an increase of OVA-specific CD8 T-cell proliferation (**b**) and IFN-γ production (**c**) were then evaluated. (**b**) Proportion of tetramer-positive cells/CD8 T cells in spleen and inguinal LN. (**c**) Spleen cells were stimulated with OVA (SL8) or WT1 (Db126) peptide for 3 days and the level of IFN-γ in the culture supernatant was measured using a CBA. NS, no significant (>0.05), $*P<0.05$, $**P<0.01$, compared with PBS control (ANOVA with Dunnett's test). (**d**) cM362-140 + OVA induced Ag-specific CTL activation via the TICAM-1 pathway. Wild-type or *Ticam1*$^{-/-}$ mice were injected s.c. with PBS, OVA or OVA + cM362-140 as described above. Spleen cells were harvested 4 days after the last adjuvant injection and OVA-specific IFN-γ productions were assessed. PBS or OVA injection did not induce IFN-γ production from spleen cells. The data from OVA + cM362-140 injection are shown. $*P<0.05$ (Student's *t*-test).

agonists, have been tested in humans[1,6], they have not yet been clinically approved because of their undesired effects.

In this study, we designed many nucleotide adjuvants and tested their functional properties. Our approach is timely since most dsRNA receptors have been identified in the mouse and

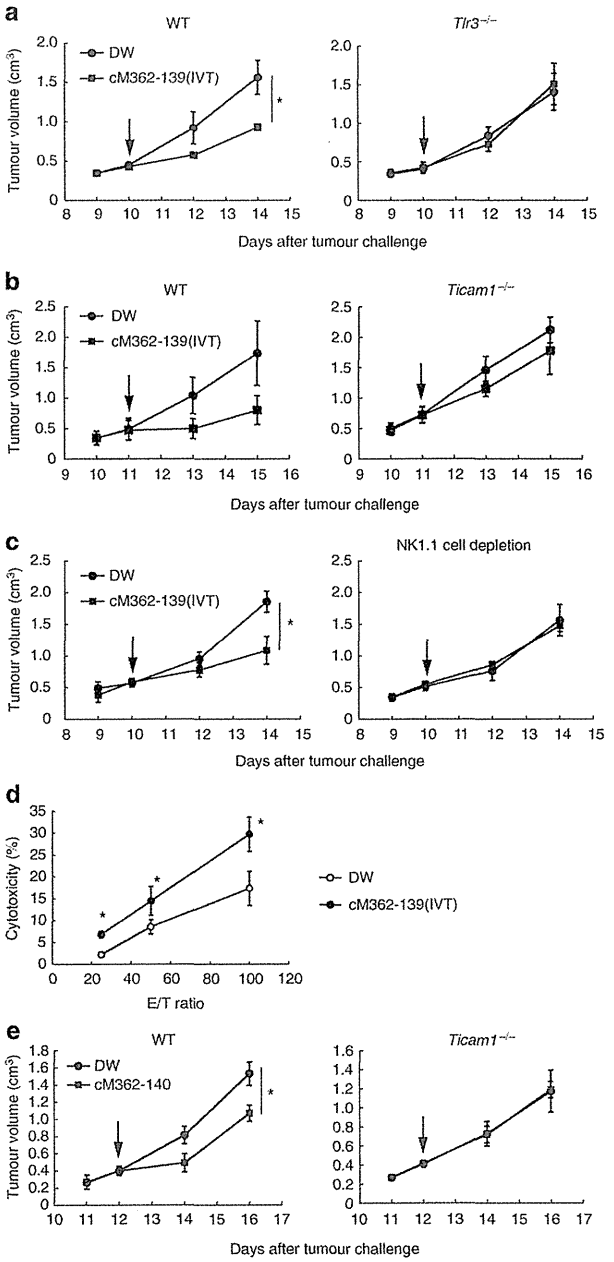

Figure 7 | Therapeutic effects of sODN-dsRNA in B16 tumour-implant model. (**a**,**b**) B16 tumour growth in mice after cM362-139(IVT) treatment. B16 melanoma cells were s.c. implanted into B6 WT mice (**a** and **b**), *Tlr3*$^{-/-}$ mice (**a**), or *Ticam1*$^{-/-}$ mice (**b**). cM362-139(IVT) or distilled water was injected s.c. around the tumour on the day indicated by arrow and then tumour volume was measured. Data are shown as tumour average volume ± s.e.; $n=3$ mice per group. $*P<0.05$. (**c**) Effect of NK cell depletion on cM362-139(IVT) treatment. Tumour-bearing mice were injected with anti-NK1.1 antibody to deplete NK cells. After 24 h, cM362-139(IVT) or distilled water was injected into the mice as described in **a**. (**d**) Cytotoxic activity of DX5^{+} NK cells isolated from cM362-139(IVT)-treated mice. DX5^{+} cells were isolated from B16 tumour-bearing mice treated with cM362-139(IVT) or distilled water for 18 h. Cytotoxic activity of DX5^{+} cells against B16 target cells was measured by ^{51}Cr release assay. (**e**) B16 tumour growth in mice after cM362-140 treatment. Tumour-bearing mice were treated with cM362-140 as described in **a**.

human[1–4], and their structures and properties have been known for a decade[32–34]. Based on our current understanding of the dsRNA response, poly(I:C) activates both TICAM-1 (ref. 35) and MAVS pathways[36] resulting in systemic cytokinemia in mice[21,37]. Viral replication intermediates, double-stranded RNA and 5′-triphosphate RNA cause activation of the RLR pathway and robust cytokine production[38,39]. Here we chemically synthesized and tested a synthetic compound, cM362-140, an sODN-dsRNA that entered the endosomes and activated the TLR3/TICAM-1 pathway *in vivo*. Specifically, cM362-140 activated TLR3 in myeloid cells, including DCs in draining LNs, and induced activation of NK cells and proliferation of CTL. There was no systemically significant production of cytokines, including IFNs, after treatment with cM362-140. Our study establishes the proof-of-concept that modified or complexed RNA can regulate the immune response through TLR3 (refs 37,40), and that cM362-140 performs this function *in vivo*.

In this study, a systemic increase in the cytokine levels was not required for the induction of an antitumour immune response. Instead, a basal cytokine level effectively primed DCs to activate tumoricidal NK cells and CTL response. Subcutaneous or i.p. injection of cM362-140 barely activated the RLR pathway, whereas poly(I:C) activated this pathway to induce systemic cytokinemia. cM362-140 activated TICAM-1 for DC maturation, but barely induced chemokine production or necroptosis in tumour cells (Supplementary Fig. 10), which were reported as a direct action of poly(I:C)[29,30]. Therefore, cM362-140 eliminates major inflammatory responses caused by poly(I:C).

The 5′-sODN sequence of cM362-140 targeted the dsRNA to the endosome and evaded recognition by RIG-I/MDA5. A 140-bp stretch of dsRNA was required for TLR3 multimerization and TICAM-1 activation, but unsatisfactory for endosome targeting[40,41]. The 5′-sODN sequence of cM362 does not contain a CpG motif, which stimulates cytokine production via TLR9 in plasmacytoid DC. To prevent Dicer-mediated RNA interference, RNA sequences specific to human mRNAs were not employed. In addition, the antisense 5′-end of cM362-140 was OH, neither phosphorylated nor capped, unlike viral or host RNA products. Although cM362-140 was an artificial compound to circumvent host innate sensors, its constituents are native and modifiable to maximize antitumour response. Although the nucleic acid-sensing system differs somewhat between mouse and human[2,4]: generally, human BDCA3$^+$ DCs express a high level of TLR3 but no TLR9 (ref. 20), whereas mouse CD8α^+ DCs express TLR3 and TLR9 (refs 2,18,41), extrapolating results from the mouse and applying them to the human will be crucial for establishing human immunotherapy in the future.

Type I IFNs have remarkable antiviral and antitumour properties, but sometimes elicit severe side effects during treatment in patients. For example, s.c. injection of poly(I:C) induces inflammation, erythema and fever[42]. In clinical trials, cancer patients cannot tolerate high doses of poly(I:C), even if administered via s.c. injection[11,42–44]. Poly(I:C) consists of polyI and polyC chains of variable lengths that differ in function from one batch to the next, and, for unknown reasons, exogenous poly(I:C) activates cytoplasmic RNA sensors[36]. By contrast, cM362-140 is uniform. It binds TLR3 and fails to activate cytoplasmic RNA sensors, indicating that immune modulation by RNA occurs only in the draining LNs and tumour microenvironment[45]. Thus, cM362-140 enables us with a 'defined' immunotherapy to patients without systemic cytokine response or inflammation.

Several compounds that activate the TICAM-1 pathway are clinically available. Monophosphoryl lipid A is a TLR4 adjuvant that activates the TICAM-2/TICAM-1 cascade via TLR4/MD-2 (ref. 46). However, monophosphoryl lipid A still retains the TLR4-mediated MyD88 activation, which conceptually different from sODN-dsRNA that activates a single cascade of PRR. Although poly(A:U) mildly activates the TLR3 pathway and induces type I IFN in humans[47], it has far less adjuvancy than poly(I:C)[6,28,48]. In a short-term clinical trial, poly(I:C$_{12}$U), also known as ampligen, has been shown to be less toxic than other immunotherapies[49,50]. Unfortunately, data on its uniformity and TLR3-specificity as an adjuvant are scant. Poly(I:C)LC, another antitumour adjuvant, has shown clinical promise, but it causes cytokine toxicity, thereby precluding its further development[5,6,42–44,51]. Type I IFN induction and the output of IFNAR activation appear to be predominant in low-dose poly(I:C) administration in human volunteers[42]. In another clinical study, a low dose (1.4 mg per body) of poly(I:C)LC in combination with NY-Eso-1, which contains TAA epitopes, has been shown to mount a tumour-specific T-cell response[11]. Although low doses of poly(I:C)LC induce type I IFN, it only insufficiently stimulates T-cell proliferation *in vivo*[11]. cM362-140 is advantageous over poly(I:C)LC in that a high dose can be used to specifically activate TICAM-1, but not MAVS *in vivo*. This is the first report of the successful chemical creation of a long, sequence-defined and bioactive TLR3-specific ligand.

The targeting of programmed cell death-1 and cytotoxic T-lymphocyte-associated protein-4 with monoclonal antibodies in patients with progressive-staged cancer may provide another immunotherapy breakthrough[52]. Except for an alum adjuvant that can induce a Th2 response[2,53], there is no suitable adjuvant-TAA combination for immunotherapy. Immune enhancing by adjuvant would be required since tumour cells can undergo mutations and survive to circumvent immune attack. A main problem is that current adjuvant candidates are all inflammatory, facilitating formation of tumour-supporting microenvironment, that accelerates genome instability, tumour growth and progression[45]. Here, sODN-dsRNA is a non-inflammatory adjuvant sustaining DC-mediated NK/CTL activation, its combining with TAAs will bring a therapeutic benefit to a number of patients with intractable tumours.

Methods

Cell culture, reagents and plasmid. HEK293 cells were maintained in Dulbecco's Modified Eagle's medium (Invitrogen) supplemented with 10% heat-inactivated FCS (Invitrogen) and antibiotics. HeLa cells were kindly provided by Dr T. Fujita (Kyoto University) and maintained in Eagle's minimal essential medium (Nissui,) supplemented with 1% L-glutamine and 5% FCS. B16D8 melanoma cells were cultured at 37 °C under 5% CO_2 in RPMI containing 10% FCS, penicillin and streptomycin. EG7 and C1498 cells were purchased from ATCC and cultured in RPMI-1640 supplemented with 10% FCS, 55 μM 2-mercaptoethanol (2-ME) and 1 mM sodium pyruvate, and RPMI-1640 supplemented with 10% FCS and 25 ng ml^{-1} 2-ME, respectively. Poly(I:C) was purchased from Amersham Biosciences. Endotoxin-free ovalbumin was purchased from Hyglos. $OVA_{257-264}$ peptide (SL8), control WT1 peptide (Db126) and OVA ($H2K^b$-SL8) tetramer were from MBL. Human serum type AB was from Lonza. ODNs were synthesized by GeneDesign. Following antibodies were used in this study: Alexa Fluor-568-conjugated secondary antibody (Invitrogen), FITC-CD8α (53-6.7) and APC-CD3ε (145-2C11) (BioLegend), and PerCP/Cy5.5-7AAD (BD Biosciences). The human TLR3 expression plasmid was constructed in our laboratory[33].

Preparation of *in vitro* transcribed sODN-dsRNAs. The leader-trailer sequence of a MV laboratory-adapted strain of Edmonston was used as the dsRNA template[25]. DNA fragments covering this region of the MV genome and the T7 promoter sequence were amplified using PCR with specific primers and the plasmid pCR-T7 MV as a template. Sense and antisense MV RNAs from the PCR products were *in vitro* transcribed using an AmpliScribe T7 transcription kit (Epicentre Technologies) according to the manufacturer's protocol. The transcribed products were purified by 8% PAGE containing 7 M urea. After visualization by ultraviolet illumination, the appropriate bands were excised and eluted with 0.3 M sodium acetate. The eluted RNAs were ethanol precipitated and resuspended in RNase-free water. For large-scale preparation of RNAs, electro-elutions were performed using D-Tube Dialyzer Maxi (Novagen) and eluted RNAs were dialyzed, concentrated and precipitated with ethanol. The concentration of RNA was determined by measuring the absorbance at 260 nm in a

spectrophotometer. To generate sODN-dsRNA, sODN + linker DNA, sense and antisense RNA were mixed and annealed. sODNs, MV RNA sequences in sODN-dsRNA and PCR primers used in this study are described in Supplementary Tables 1–3.

Preparation of cM362-140. The chemically synthesized long RNAs as an alternative to *in vitro* transcribed RNAs were completed by a ligation reaction mediated by splint DNA[54] with slight modification. The outline of chemical synthesis was described below.

To prepare the sense strand of cM362-140, the ligation reactions were performed in two steps. First, S2 RNA (40 nmol), S3 RNA (40 nmol) and specific splint DNA (40–48 nmol) were mixed, heated at 90 °C for 5 min and slowly cooled to 4 °C (Supplementary Table 4A,B). Following hybridization, T4 DNA ligase (Takara) was added and incubated at room temperature for 16–22 h. The ligation reaction mixtures comprised 15.4 μM annealed complex, 66 mM Tris-HCl (pH 7.6), 6.6 mM $MgCl_2$, 10 mM DTT, 0.1 mM ATP and ~31 U μl^{-1} T4 DNA ligase. As the second ligation, S1 cM362-RNA (40 nmol) and the specific splint DNA (40–48 nmol) for the second ligation site were added into the first ligation reaction mixture, hybridized and T4 DNA ligase was added. The mixture was incubated at room temperature for 16–22 h. The derived full-length 165 mer sense strand was isolated by 8% PAGE containing 7 M urea and electro-elution. The subsequent procedure was the same as described in the section describing purification of *in vitro* transcribed RNAs. Overall yield was 8–10%.

To prepare the antisense RNA of cM362-140, three fragment RNAs, AS1, AS2 and AS3 (33 nmol each) and the related splint DNAs (33 nmol each) were mixed, hybridized and then T4 DNA ligase was added. The mixture was incubated at room temperature for 16–22 h. The following procedure was the same as described above. Overall yield was 15–22%. To generate cM362-140, sense- and antisense-RNAs were annealed.

Analysis with microchip electrophoresis. To analyse the cM362-139 complex, we used a microchip electrophoresis instrument (model SV1210; Hitachi Electronics Engineering Co. Ltd.). The standard procedure for electrophoresis using 2-mercaptoethanol (ME) has been previously described[55,56]. sODN or RNAs were adjusted to 0.2 μM with water. The sODN/RNA1/RNA2 complex (designated cM362-139) and dsRNA (RNA1 + RNA2) were prepared by mixing DNA or RNAs and hybridizing in water (final concentration 0.4 μM). The sample solution (10 μl) was applied to the sample well of the microchip device and the programme was run at 600 V for 120 s (injection time), then at 1,100 V for 180 s (separation time) under 350 V of return voltage at 20 °C. During the electric separation, DNA or RNA peaks were detected by laser induced fluorescence and analysed.

Agarose gel electrophoresis. cM362-139(IVT) and cM362-140 were incubated in PBS or in RNase-free water with or without serum, for 60 min at 37 °C or 42 °C. Aliquots containing 0.1–0.2 μg of incubated sODN-dsRNAs were then mixed with 10 × loading dye (Takara Bio Inc.) and loaded onto 3 or 4% agarose gel (Nusieve 3:1 Agarose, Lonza) containing ethidium bromide. After electric separation, nucleic complexes were visualized using ultraviolet transilluminator (FAS-III, Toyobo).

Reporter gene assay. HEK293 cells (8×10^5 cells per well) were cultured in six-well plates and transfected with the TLR3 expression vector or empty vector (400 ng per well) together with the reporter plasmid (400 ng per well) and an internal control vector, phRL-TK (Promega; 20 ng per well) using Lipofectamine 2000 (Invitrogen). The p-125 luc reporter containing the human IFN-β promoter region (−125 to +19) was provided by Dr T. Taniguchi (University of Tokyo). Twenty-four hours after transfection, cells were collected and resusupended in medium with or without FCS. Then, cells were seeded into 96-well plates and stimulated with the indicated RNAs for 6 h. The *Firefly* and *Renilla* luciferase activities were determined using a dual-luciferase reporter assay kit (Promega). The *Firefly* luciferase activity was normalized to the *Renilla* luciferase activity and was expressed as the fold induction relative to the activity in unstimulated vector-transfected cells. All assays were performed in triplicate.

Cytokine assay. Splenic $CD11c^+$ DCs from wild-type, $Tlr3^{-/-}$ or $Mavs^{-/-}$ mice were prepared as described previously[9,31]. Cells were suspended in RPMI-1640 (Invitrogen) supplemented with 10% heat-inactivated FCS and antibiotics and stimulated with the indicated RNAs. Twenty-four hours after stimulation, culture supernatants were collected and analysed for cytokine levels by ELISA or Cytometric Bead Array (CBA). ELISA kits for mouse IFN-α and IFN-β were purchased from PBL Biomedical Laboratories. CBA flex sets for mouse IL-6 and TNF-α were purchased from BD Bioscience. Experiments were performed according to the manufacturer's instructions and samples were analysed using the Facs Aria (BD Bioscience).

Confocal microscopy. HeLa cells (1.0×10^5 cells per well) were cultured on microcover glasses (Matsunami Glass Ind., Ltd) in a 12-well plate. Three hours after seeding, cells were transfected with GFP-fused Rab5a or Lamp1 using BacMam systems (Cell Light Early Endosomes-GFP BacMam 2.0 or Cell Light Lysosomes-GFP BacMam 2.0, Life technologies) or left untreated. Sixteen hours after transfection, cells were incubated with 15 μg ml^{-1} Cy3-labelled cM362, cM362-dsRNAs or dsRNAs for 30 min at 4 °C. Cells were washed twice and further incubated at 37 °C. And then, cells were fixed with 4% paraformaldehyde at the time points indicated. The coverslips were mounted onto slide glass with Prolong Gold with DAPI for nuclei staining. Cells were visualized at a × 63 magnification using a Zeiss LSM520 META microscope (Carl Zeiss Microscopy GmbH).

Quantitative PCR (qPCR). Total RNA was extracted using the Trizol reagent (Qiagen) and reverse-transcribed using a high-capacity cDNA Reverse Transcripition kit (Applied Biosystems) and random primers according to the manufacturer's instructions. QPCR was performed using specific primers for mouse *GAPDH, IFN-β, IL-6* and *TNF-α* (Supplementary Table 5) and the Step One Real-time PCR system (Applied Biosystems).

Mice. $Ticam1^{-/-}$ and $Mavs^{-/-}$ mice were made in our laboratory and back-crossed more than eight times to adapt C57BL/6 background[9,10]. Inbred C57BL/6 WT mice were purchased from CLEA Japan. $Tlr3^{-/-}$ mice were kindly provided by Dr S. Akira (Osaka University). Mice were maintained under specific pathogen-free conditions in the animal facility of the Hokkaido University Graduate School of Medicine. Female mice 6–12 weeks of age were used in all experiments, all of which were performed according to the guidelines issued by the Hokkaido University Animal Care and Use Committee.

***In vivo* mouse cytokine assay.** Wild-type and $Tlr3^{-/-}$ mice (9 weeks) were injected i.p. with 50 μl (50 μg) poly(I:C), cM362-139 (IVT) or cM362-140, and blood was collected from the tail vein at timed intervals. Cytokine levels in sera were measured using a CBA. In some cases, wild-type and $Ticam1^{-/-}$ mice were s.c. injected with 75 μl (75 μg) poly(I:C) or cM362-140. After 6 h, mice were killed and draining inguinal LN, axillary LN and spleen were harvested[10]. *IFN-β, IL-6* or *TNF-α* mRNA expression in these lymphoid organs was measured by qPCR.

Tumour challenge and sODN-dsRNA treatment. Mice 6–10 weeks of age were used in all experiments. Mice were shaved at the back and injected s.c. with 200 μl of 6×10^5 B16D8 cells in PBS (−). Tumour volumes were measured at regular intervals using a caliper[9]. Tumour volume was calculated using the following formula: tumour volume (cm^3) = (long diameter) × (short diameter)^2 × 0.4. 75 μl (75 μg) sODN-dsRNAs or distilled water with no detectable LPS was mixed with *in vivo*-JetPEI (Polyplus), a polymer-based transfection reagent, according to the manual and then injected s.c. around the tumour. Treatment was started when the average tumour volume of 0.4–0.6 cm^3 was reached. To deplete NK cells, we injected titrated anti-NK1.1 ascites (PK136) i.p. in tumour-bearing mice the day before sODN-dsRNA treatment. Depletion of $NK1.1^+$ cells was verified by flow cytometory.

In the case of EG7 cell challenge, mice were injected s.c. with 200 μl of 2×10^6 syngenic EG7 cells in PBS (−). When the average tumour volumes reached ~0.6 cm^3, 50 μl of 100 μg endotoxin-free ovalbumin in PBS (−) with or without 50 μl of 50 μg poly(I:C) or sODN-dsRNA was injected s.c. around the tumour. PBS (−) (100 μl) was used as a control. Treatments were performed twice per week.

CTL activity in tumour-bearing mice after adjuvant therapy. Female mice 6–10 weeks of age were used for this study. Splenocytes were harvested from tumour-bearing mice at 7 days after the last adjuvant treatment. In the case of tumour-free settings, spleen and inguinal LN cells were harvested from wild-type or $Ticam1^{-/-}$ mice 4 days after the last adjuvant injection. The cells were stained with FITC-CD8α (1:200), PerCP/Cy5.5-7AAD (1:200), APC-CD3ε (1:200) and PE-OVA-tetramer (1:50) to detect Ag-specific $CD8^+$ T cells. To evaluate cytokine production, splenocytes (2×10^6 per 200 μl per well) were cultured for 3 days in the presence of 100 nM OVA peptide (SL8: SIINFEKL) or control WT1 peptide (Db126: RMFPNAPYL) and IFN-γ production was analysed with CBA or ELISA. To assess the cytotoxic activity of CTLs, splenocytes (1×10^6 per ml) were co-cultured with mitomycin C-treated EG7 cells (5×10^5 per ml) in the presence of 10 U ml^{-1} IL-2 for 5 days. Then, the cells were incubated with ^{51}Cr-labelled EG7 or C1498 cells for 4 h and determined cytotoxic activity[10]. The cytotoxicity was calculated by this formula: Cytotoxicity (%) = [(experimental release − spontaneous release)/(total release—spontaneous release)] × 100.

Cytotoxic activity assay of NK cells. Mice bearing B16 tumour were injected s.c. with cM362-139(IVT) mixed with *in vivo*-JetPEI. After 18 h, mice were killed and $DX5^+$ NK cells were isolated from spleen using DX5-positive selection microbeads (Miltenyi) according to the manual[9]. B16 cells were labelled with ^{51}Cr for 1 h and then washed three times with medium. $DX5^+$ cells and ^{51}Cr-labelled B16 cells were co-cultured at the indicated ratio[31]. After 4 h, supernatants were harvested and ^{51}Cr release was measured in each sample. Specific lysis was calculated by the following formula: cytotoxicity (%) = [(experimental release − spontaneous release)/(total release − spontaneous release)] × 100.

Statistical analysis. The significance of differences between groups was determined by the Student's *t*-test. In tumour-implant or -free mouse experiments, one-way analysis of variance with Bonferroni's multiple-comparison test or Dunnett's test was performed to analyse statistical significance.

References

1. Akira, S., Uematsu, S. & Takeuchi, O. Pathogen recognition and innate immunity. *Cell* **124,** 783–801 (2006).
2. Gürtler, C. & Bowie, A. G. Innate immune detection of microbial nucleic acids. *Trends Microbiol.* **21,** 413–420 (2013).
3. Seya, T. *et al.* Role of Toll-like receptors and their adaptors in adjuvant immunotherapy for cancer. *Anticancer Res.* **23,** 4369–4376 (2003).
4. Matsumoto, M. & Seya, T. TLR3: interferon induction by double-stranded RNA including poly(I:C). *Adv. Drug Deliv. Rev.* **60,** 805–812 (2008).
5. Levine, A. S. & Levy, H. B. Phase I-II trials of poly IC stabilized with poly-L-lysine. *Cancer Treat. Rep.* **62,** 1907–1912 (1978).
6. Galluzzi, L. *et al.* Trial watch: experimental Toll-like receptor agonists for cancer therapy. *OncoImmunology* **1,** 699–716 (2012).
7. Lvovsky, E. A., Mossman, K. L., Levy, H. B. & Dritschilo, A. Response of mouse tumor to interferon inducer and radiation. *Int. J. Radiat. Oncol. Biol. Phys.* **11,** 1721–1725 (1985).
8. Talmadge, J. E. *et al.* Immunotherapeutic potential in murine tumor models of polyinosinic-polycytidylic acid and poly-L-lysine solubilized by carboxymethyl cellulose. *Cancer Res.* **45,** 1066–1072 (1985).
9. Akazawa, T. *et al.* Antitumor NK activation induced by the Toll-like receptor 3-TICAM-1 (TRIF) pathway in myeloid dendritic cells. *Proc. Natl Acad. Sci. USA* **104,** 252–257 (2007).
10. Azuma, M., Ebihara, T., Oshiumi, H., Matsumoto, M. & Seya., T. Cross-priming for antitumor CTL induced by soluble Ag + polyI:C depends on the TICAM-1 pathway in mouse CD11c(+)/CD8α(+) dendritic cells. *Oncoimmunology* **1,** 581–592 (2012).
11. Sabbatini, P. *et al.* Phase I trial of overlapping long peptides from a tumor self-antigen and poly-ICLC shows rapid induction of integrated immune response in ovarian cancer patients. *Clin. Cancer Res.* **18,** 6497–6508 (2012).
12. Yoneyama, M., Onomoto, K. & Fujita, T. Cytoplasmic recognition of RNA. *Adv. Drug Deliv. Rev.* **60,** 841–846 (2008).
13. Dixit, E. & Kagan, J. C. Intracellular pathogen detection by RIG-I-like receptors. *Adv. Immunol.* **117,** 99–125 (2013).
14. Matsumoto, M. *et al.* Subcellular localization of Toll-like receptor 3 in human dendritic cells. *J. Immunol.* **171,** 3154–3162 (2003).
15. Sun, J. C., Beilke, J. N. & Lanier, L. L. Adaptive immune features of natural killer cells. *Nature* **457,** 557–561 (2009).
16. Fernandez, N. C. *et al.* Dendritic cells directly trigger NK cell functions: cross-talk relevant in innate anti-tumor immune responses in vivo. *Nature Med.* **5,** 405–411 (1999).
17. Schulz, O. *et al.* Toll-like receptor 3 promotes cross-priming to virus-infected cells. *Nature* **433,** 887–892 (2005).
18. Villadangos, J. A. & Shortman, K. Found in translation: the human equivalent of mouse CD8 + dendritic cells. *J. Exp. Med.* **207,** 1131–1134 (2010).
19. Edelson, B. T. *et al.* Peripheral CD103 + dendritic cells form a unified subset developmentally related to CD8alpha + conventional dendritic cells. *J. Exp. Med.* **207,** 823–836 (2010).
20. Jongbloed, S. L. *et al.* Human CD141 + (BDCA-3) + dendritic cells (DCs) represent a unique myeloid DC subset that cross-presents necrotic cell antigens. *J. Exp. Med.* **207,** 1247–1260 (2010).
21. Kato, H. *et al.* Differential roles of MDA5 and RIG-I helicases in the recognition of RNA viruses. *Nature* **441,** 101–105 (2006).
22. Okahira, S. *et al.* Interferon-beta induction through Toll-like receptor 3 depends on double-stranded RNA structure. *DNA Cell Biol.* **24,** 614–623 (2005).
23. Itoh, K., Watanabe, A., Funami, K., Seya, T. & Matsumoto, M. The clathrin-mediated endocytic pathway participates in dsRNA-induced IFN-beta production. *J. Immunol.* **181,** 5522–5529 (2008).
24. Liu, L. *et al.* Structural basis of Toll-like receptor 3 signaling with double-stranded RNA. *Science* **320,** 379–381 (2008).
25. Shingai, M. *et al.* Differential type I IFN-inducing abilities of wild-type versus vaccine strains of measles virus. *J. Immunol.* **179,** 6123–6133 (2007).
26. Miyake, T. *et al.* Poly I:C-induced activation of NK cells by CD8 alpha + dendritic cells via the IPS-1 and TRIF-dependent pathways. *J. Immunol.* **183,** 2522–2528 (2009).
27. Zhang, Z. *et al.* DDX1, DDX21, and DHX36 helicases form a complex with the adaptor molecule TRIF to sense dsRNA in dendritic cells. *Immunity* **34,** 866–878 (2011).
28. Gauzzi, M. C., Del Cornò, M. & Gessani, S. Dissecting TLR3 signalling in dendritic cells. *Immunobiology* **215,** 713–723 (2010).
29. Conforti, R. *et al.* Opposing effects of Toll-like receptor (TLR3) signaling in tumors can be therapeutically uncoupled to optimize the anticancer efficacy of TLR3 ligands. *Cancer Res.* **70,** 490–500 (2010).
30. Paone, A. *et al.* Toll-like receptor 3 triggers apoptosis of human prostate cancer cells through a PKC-alpha-dependent mechanism. *Carcinogenesis* **29,** 1334–1342 (2008).
31. Ebihara, T. *et al.* Identification of a polyI:C-inducible membrane protein that participates in dendritic cell-mediated natural killer cell activation. *J. Exp. Med.* **207,** 2675–2687 (2010).
32. Alexopoulou, L., Holt, A. C., Medzhitov, R. & Flavell, R. A. Recognition of double stranded RNA and activation of NF-kappaB by Toll-like receptor 3. *Nature* **413,** 732–738 (2001).
33. Matsumoto, M., Kikkawa, S., Kohase, M., Miyake, K. & Seya, T. Establishment of a monoclonal antibody against human Toll-like receptor 3 that blocks double-stranded RNA-mediated signaling. *Biochem. Biophys. Res. Commun.* **293,** 1364–1369 (2002).
34. Shime, H. *et al.* Toll-like receptor 3 signaling converts tumor-supporting myeloid cells to tumoricidal effectors. *Proc. Natl. Acad. Sci. U. S. A.* **109,** 2066–2071 (2012).
35. Oshiumi, H., Matsumoto, M., Funami, K., Akazawa, T. & Seya, T. TICAM-1, an adaptor molecule that participates in Toll-like receptor 3-mediated interferon-beta induction. *Nat. Immunol.* **4,** 161–167 (2003).
36. Yoneyama, M. *et al.* The RNA helicase RIG-I has an essential function in double-stranded RNA-induced innate antiviral responses. *Nat. Immunol.* **5,** 730–737 (2004).
37. Seya, T., Azuma, M. & Matsumoto, M. Targeting TLR3 with no RIG-I/MDA5 activation is effective in immunotherapy for cancer. *Expert Opin. Ther. Targets.* **17,** 533–544 (2013).
38. Hornung, V. *et al.* RNA is the ligand for RIG-I. *Science* **314,** 994–997 (2006).
39. Pichlmair, A. *et al.* RIG-I-mediated antiviral responses to single-stranded RNA bearing 5′-phosphates. *Science* **314,** 997–1001 (2006).
40. Tatematsu, M., Nishikawa, F., Seya, T. & Matsumoto, M. Toll-like receptor 3 recognizes incomplete stem structures in single-stranded viral RNA. *Nat. Commun.* **4,** 1833 (2013).
41. Jelinek, I. *et al.* TLR3-specific double-stranded RNA oligonucleotide adjuvants induce dendritic cell cross-presentation, CTL responses, and antiviral protection. *J. Immunol.* **186,** 2422–2429 (2011).
42. Caskey, M. *et al.* Synthetic double-stranded RNA induces innate immune responses similar to a live viral vaccine in humans. *J. Exp. Med.* **208,** 2357–2366 (2011).
43. Levy, H. B., Low, L. W. & Rabson, A. S. Inhibition of tumor growth by polyinosinic-polycytidylic acid. *Proc. Natl Acad. Sci. USA* **62,** 357–361 (1969).
44. Levine, A. S., Sivulich, M., Wiernik, P. H. & Levy, H. B. Initial clinical trials in cancer patients of polyriboinosinic-polyribocytidylic acid stabilized with poly-L-lysine, in carboxymethylcellulose [poly(ICLC)], a highly effective interferon inducer. *Cancer Res.* **39,** 1645–1650 (1979).
45. Lin, W. W. & Karin, M. A cytokine-mediated link between innate immunity, inflammation, and cancer. *J. Clin. Invest.* **117,** 1175–1183 (2007).
46. Mata-Haro, V. *et al.* The vaccine adjuvant monophosphoryl lipid A as a TRIF-biased agonist of TLR4. *Science* **316,** 1628–1632 (2007).
47. Sugiyama, T. *et al.* Immunoadjuvant effects of polyadenylic:polyuridylic acids through TLR3 and TLR7. *Int. Immunol.* **20,** 1–9 (2008).
48. Perrot, I. *et al.* TLR3 and Rig-like receptor on myeloid dendritic cells and Rig-like receptor on human NK cells are both mandatory for production of IFN-gamma in response to double-stranded RNA. *J. Immunol.* **185,** 2080–2088 (2010).
49. Gowen, B. B. *et al.* TLR3 is essential for the induction of protective immunity against Punta Toro Virus infection by the double-stranded RNA (dsRNA), poly(I:C12U), but not Poly(I:C): differential recognition of synthetic dsRNA molecules. *J. Immunol.* **178,** 5200–5208 (2007).
50. Jasani, B., Navabi, H. & Adams, M. Ampligen: a potential toll-like 3 receptor adjuvant for immunotherapy of cancer. *Vaccine* **27,** 3401–3404 (2009).
51. Hafner, A. M., Corthésy, B. & Merkle, H. P. Particulate formulations for the delivery of poly(I:C) as vaccine adjuvant. *Adv. Drug Deliv. Rev.* **65,** 1386–1399 (2013).
52. Intlekofer, A. M. & Thompson, C. B. At the bench: preclinical rationale for CTLA-4 and PD-1 blockade as cancer immunotherapy. *J. Leukoc. Biol.* **94,** 25–39 (2013).
53. Desmet, C. J. & Ishii, K. J. Nucleic acid sensing at the interface between innate and adaptive immunity in vaccination. *Nat. Rev. Immunol.* **12,** 479–491 (2012).
54. Jing, X. u., Lapham, J. & Crothers, D. M. Determining RNA solution structure by segmental isotopic labeling and NMR: Application to *Caenorhabditis elegans* spliced leader RNA 1. *Proc. Natl Acad. Sci. USA* **93,** 44–48 (1996).
55. Nishikawa, F., Arakawa, H. & Nishikawa, S. Application of microchip electrophoresis in the analysis of RNA aptamer-protein interactions. *Nucleos. Nucleot. Nucl. Acids* **25,** 369–382 (2006).
56. Nishikawa, F., Murakami, K., Matsugami, A., Katahira, M. & Nishikawa, S. Structural studies of an RNA aptamer containing GGA repeats under ionic conditions using microchip electrophoresis, circular dichroism, and 1D-NMR. *Oligonucleotides* **19,** 179–190 (2009).

Acknowledgements

We are grateful to Dr H. Nankai (GeneDesign, Inc., Osaka) for helping chemical synthesis of RNA. Technical and clerical assistance by Dr R. Hatsugai, and Ms H. Sato in our laboratory is gratefully acknowledged. We appreciate Dr K. Toyoshima (RIKEN, Tokyo) for organizing the start of this project.

Author contributions

M.M. and T.S. conceived and designed the experiments. M.T., F.N., M.A., N.I., A.M.-S. and H.S. performed the experiments. M.M. conducted the project. M.M. and T.S. analysed data and wrote the paper.

Additional information

Supplementary Information accompanies this paper at http://www.nature.com/naturecommunications

Competing financial interests: The authors declare no competing financial interests.

Reprints and permission information is available online at http://npg.nature.com/reprintsandpermissions/

How to cite this article: Matsumoto, M. *et al.* Defined TLR3-specific adjuvant that induces NK and CTL activation without significant cytokine production *in vivo*. *Nat. Commun.* 6:6280 doi: 10.1038/ncomms7280 (2015).

Biochemical and Biophysical Research Communications 457 (2015) 445–450

Contents lists available at ScienceDirect

Biochemical and Biophysical Research Communications

journal homepage: www.elsevier.com/locate/ybbrc

Pam2 lipopeptides systemically increase myeloid-derived suppressor cells through TLR2 signaling

Akira Maruyama [1], Hiroaki Shime*, [1], Yohei Takeda, Masahiro Azuma, Misako Matsumoto, Tsukasa Seya*

Department of Microbiology and Immunology, Hokkaido University Graduate School of Medicine, Kita 15, Nishi 7, Kita-ku, Sapporo 060-8638, Japan

ARTICLE INFO

Article history:
Received 24 December 2014
Available online 13 January 2015

Keywords:
Myeloid-derive suppressor cells (MDSCs)
Pam2 lipopeptides
Toll-like receptor 2
Immunosuppression
Antitumor immunotherapy

ABSTRACT

Myeloid-derived suppressor cells (MDSCs) are immature myeloid cells that exhibit potent immunosuppressive activity. They are increased in tumor-bearing hosts and contribute to tumor development. Toll-like receptors (TLRs) on MDSCs may modulate the tumor-supporting properties of MDSCs through pattern-recognition. Pam2 lipopeptides represented by Pam2CSK4 serve as a TLR2 agonist to exert antitumor function by dendritic cell (DC)-priming that leads to NK cell activation and cytotoxic T cell proliferation. On the other hand, TLR2 enhances tumor cell progression/invasion by activating tumor-infiltrating macrophages. How MDSCs respond to TLR2 agonists has not yet been determined. In this study, we found intravenous administration of Pam2CSK4 systemically up-regulated the frequency of MDSCs in EG7 tumor-bearing mice. The frequency of tumor-infiltrating MDSCs was accordingly increased in response to Pam2CSK4. MDSCs were not increased by Pam2CSK4 stimuli in TLR2 knockout (KO) mice. Adoptive transfer experiments using CFSE-labeled MDSCs revealed that the TLR2-positive MDSCs survived long in tumor-bearing mice in response to Pam2CSK4 treatment. Since the increased MDSC population sustained immune-suppressive properties, our study suggests that Pam2CSK4-triggered TLR2 activation enhances the MDSC potential and suppress antitumor immune response in tumor microenvironment.

1. Introduction

TLR2 signaling pathway plays a critical role in induction of protective immunity against infection [1,2]. TLR2 enhances dendritic cell/macrophage functions that cause host defense, but exerts a controversial effect on cancer development [2]. Recent reports demonstrated that treatment with purified TLR2 ligands such as Pam2CSK4, Pam3CSK4, MALP2 or related synthetic compounds inhibited tumor growth in mice tumor implant models [3,4]. Pam2 lipopeptides trigger activation of TLR2 in combination with TLR6 or TLR1 in conventional DCs, which leads to maturation of the DCs through the MyD88-dependent signaling pathway, resulting in NK cell activation and CTL proliferation [5–7].

In tumor-bearing mice with systemic exposing to TLR2 agonists, however, an opposite effect was reported: TLR2 signal-induced inflammation may contribute to tumor progression. TLR2 is also expressed on immune cells with regulatory properties that include tumor-associated macrophages (TAMs), myeloid-derived suppressor cells (MDSCs) as well as tumor cells [8–10]. Host cell-derived endogenous TLR2 ligand, such as versican, a chondroitin sulfate proteoglycan derived from cancer cells, stimulates macrophages to produce TNF-α, which enhances lung metastasis of cancer cells [11]. Furthermore, Pam2CSK4 primes DC activation to induce expansion of $Foxp3^{+}CD25^{+}CD4^{+}$ regulatory T cells (Treg) and cause immune tolerance against cancer [12,13]. These reports suggest that TLR2 signaling may modulate the myeloid cell function, which promotes growth, invasion, or metastasis of tumor cells. There might be cell type-to-cell type difference in TLR2 response to its ligands, which critically determines their mode for regulation against tumor progression or survival.

MDSCs are heterogenous populations of immature myeloid cells that have immunosuppressive activity. MDSCs are expanded in

Abbreviations: CFSE, carboxyfluorescein succinimidyl ester; CTL, cytotoxic T lymphocyte; DAMP, damage-associated molecular pattern; DC, dendritic cell; MALP-2, macrophage activating lipopeptide-2; NK, natural killer; Pam2, 16 S-[2,3-bis(palmitoyl)propyl]cysteine; TLR, toll-like receptor.

* Corresponding authors. Fax: +81 11 706 7866.
E-mail addresses: shime@med.hokudai.ac.jp (H. Shime), seya-tu@pop.med.hokudai.ac.jp (T. Seya).

[1] The first two authors were equally contributed.

http://dx.doi.org/10.1016/j.bbrc.2015.01.011
0006-291X/

tumor-bearing mice and patients with cancer such as colon cancer, bladder cancer, lung cancer, and ovarian cancer. They impede the efficacy of cancer immunotherapy [14]. Depletion of MDSCs augments anti-tumor activity of host immune cells by restoring effector cell function [15]. Mouse MDSCs are characterized by the markers of $CD11b^{+}Gr1^{+}$. MDSCs subvert anti-tumor immunity by suppression of DC maturation, T cell proliferation and NK cell activation, and by induction of immunosuppressive M2 macrophage and Tregs [14,16,17]. MDSCs consist of $Ly6C^{high}Ly6G^{-}CD11b^{+}$ monocytic MDSCs (M-MDSCs) and $Ly6C^{low}Ly6G^{+}CD11b^{+}$ granulocytic MDSCs (G-MDSCs). Both subsets show distinct features and exert immunosuppressive activity by different mechanisms [18]. Inflammation-associated molecules induce accumulation of MDSCs and enhance immunosuppressive activity in local environment. Recent reports demonstrated that TLR signaling regulated tumor growth by modifying MDSC function [19]. MDSCs express TLRs, through which TLR ligands modify their accumulation, differentiation and function [20]. Tumor cell-derived exosomes containing Hsp72 induce expansion and suppressive activity of MDSCs through the TLR2-IL-6-STAT3 axis [9]. The S100A8/A9 complex produced in tumor regulates accumulation and suppressive activity of MDSCs through the TLR4 signaling pathway [21,22]. On the other hand, TLR9 and TLR3 ligands such as CpG ODN and poly I:C, respectively, are demonstrated to modify MDSC function directly or indirectly. Those functionally modified MDSCs exhibit loss of immunosuppressive activity against T cell function as well as act as the accessory cells for NK cell activation [23–25]. In this context, what happens in MDSCs when TLR2 agonist is exogenously administered to tumor-bearing mice remains poorly understood.

In this study, we revealed that Pam2CSK4 induces accumulation of MDSCs in spleen and tumor in tumor-bearing hosts. Pam2CSK4 can support long survival of MDSCs through the TLR2 signaling pathway.

2. Materials and methods

2.1. Mice and cells

C57BL/6J (B6 WT) female mice were obtained from CLEA Japan Inc. (Tokyo, Japan). $TLR2^{-/-}$ mice were provided by Dr. Shizuo Akira (Osaka University, Osaka, Japan). C57BL6-Tg (CAG-EGFP) mice (EGFP transgenic mice) were provided by Dr. Masaru Okabe (Osaka University). The mice were maintained in the Hokkaido University Animal Facility (Sapporo, Jappan). *Mice of 8- to 12-weeks of age* were used in all experiments that were performed according to animal experimental ethics committee guidelines of Hokkaido University. EG7 cells were purchased from ATCC and cultured in RPMI1640/10% FCS/55 μM 2-ME/1 mM sodium pyruvate/penicillin/streptomycin. B16D8 cells were established in our laboratory and cultured in RPMI1640/10% FCS/penicillin/streptomycin [26].

2.2. Reagents and antibodies

FITC-conjugated anti-CD45 (30-F11), Alexa-700 or APC-conjugated anti-CD45.2 (104), Alexa 700, FITC or PE-conjugated anti-CD11b (M1/70), biotinylated, APC-conjugated anti-Gr-1 (RB6-8C5), purified anti-CD16/CD32 (2.4G2), and isotype antibodies were obtained from Biolegend (San Diego, CA, USA). 2,3-bis (palmitoyl) propyl CSKKKK (Pam2CSK4) was synthesized by Biologica Co. Ltd (Nagoya, Japan). To rule out LPS contamination, we treated Pam2CSK4 with 200 μg/ml of polymixin B for 30 min at 37 °C before use.

2.3. Tumor models

Mice were shaved at the back and injected subcutaneously (s.c.) with EG7 cells (1×10^6) or B16D8 (6×10^5) suspended in 200 μl PBS(−). When tumor grew, tumor size was measured using a caliper. In some experiments, Pam2CSK4 was i.p. injected into tumor-bearing mice. Tumor volume was calculated using the following formula: tumor volume (cm^3) = (long diameter) × (short diameter)^2 × 0.4. Pam2CSK4 was injected intravenously (i.v.) as indicated.

2.4. Isolation of cells

Tumor-infiltrating myeloid cells were defined by gating in FACS-sorting as previously described [25,27]. $CD11b^{+}Gr1^{+}$ MDSCs were separated with anti-Gr-1 biotinylated antibody and streptavidin microbeads (Miltenyi Biotech) from spleen cell suspensions of EG7 tumor-bearing mice. The purity of isolated cells was more than 90% as assessed by flow cytometory. Almost 100% of $Gr1^{+}$ cells were $CD11b^{+}$.

2.5. Flow cytometric analysis

Cells prepared from mouse spleen, blood or tumor were blocked with anti-CD16/32 antibody and stained with fluorescent antibodies. Samples were analyzed with the FACS Calibur instrument or the FACS Aria II instrument (BD Bioscience) and data analysis was performed by the Flow Jo software (Tree Star, USA).

2.6. Cell proliferation assay

T cell proliferation was measured by changes in fluorescence intensity using CFSE. OT-I splenocytes were labeled with 1 μM CFSE for 10 min and cultured with CD11b + Gr1 + MDSC in the presence of 50 nM SL8 peptide ($OVA_{257-264}$) and/or 100 nM Pam2CSK4. After 3 days, cells were harvested, stained with APC-anti-CD8α and PE-anti-TCR vβ 5.1, 5.2 or Alexa 700-anti-CD3ε, and CFSE signal of the gated lymphocytes was analyzed with a FACS Calibur instrument or FACS Aria II instrument. The extent of cell proliferation was quantified by Flow Jo software.

2.7. Adoptive transfer

EG7 tumor-bearing mice were injected i.v. with 5×10^6 CFSE-labeled MDSCs, and then injected i.v. with 50 nmol Pam2CSK4. After 24 h, spleen cells were blocked with anti-CD16/32 antibody and stained with fluorescent antibodies. Samples were measured by flow cytometry using the FACS Aria II. Data analysis was performed using the Flow Jo software.

2.8. Statistics

If not otherwise stated, data were expressed as arithmetic means ± SD, and statistical analyses were made by 2-tailed Student's t test. $p < 0.05$ was considered statistically significant.

3. Results

3.1. Expansion of TLR2-expressing MDSCs in EG7 tumor-bearing mice

We examined TLR2 expression on MDSCs in C57BL6/J mice subcutaneously (s.c.) implanted with EG7 lymphoma cells. 21 days after tumor inoculation when tumor volumes reached 4–8 cm^3, spleen cells of the tumor-bearing mice were analyzed by flow

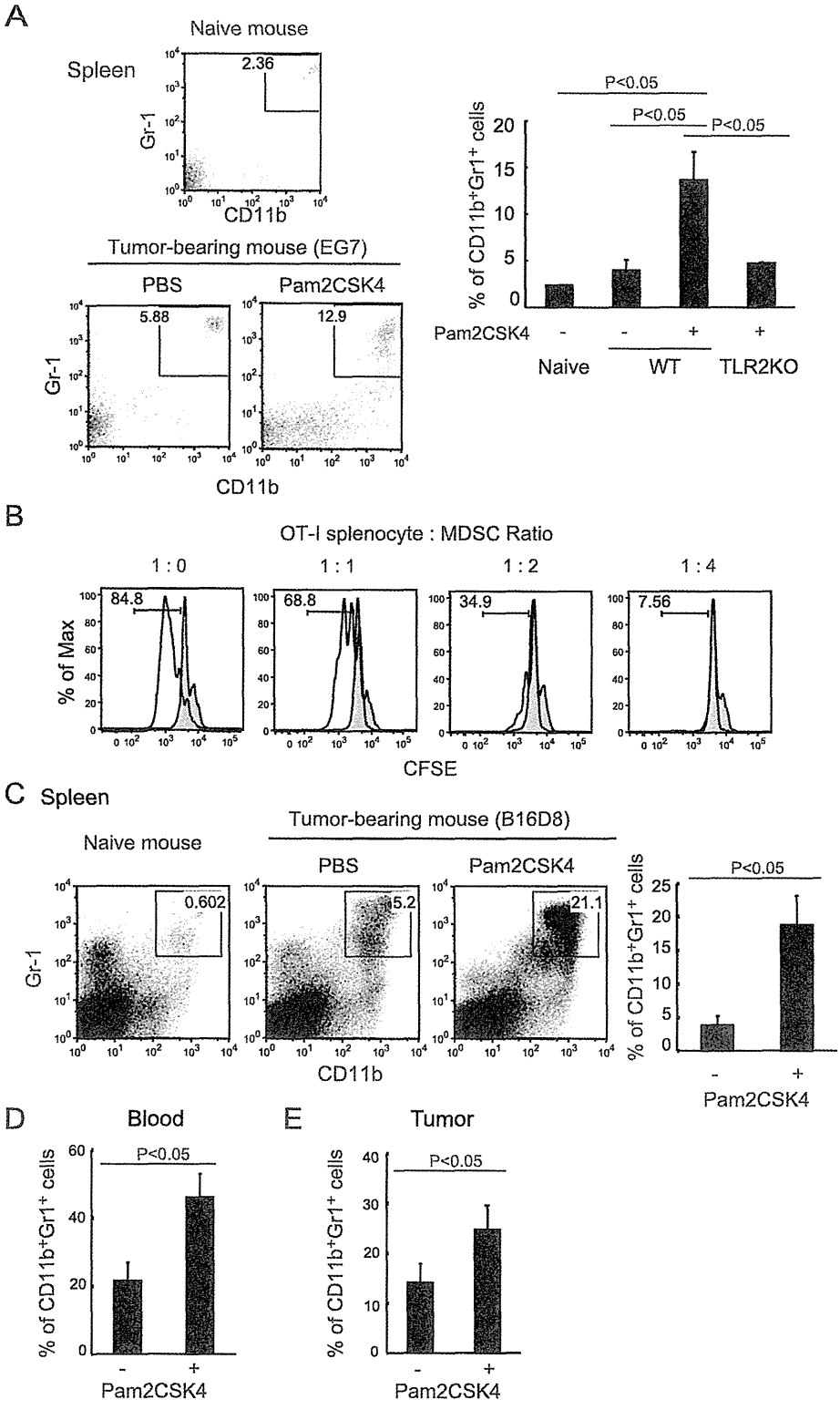

Fig. 1. Pam2CSK4 treatment induces accumulation of $CD11b^+Gr1^+$ MDSCs in tumor-bearing mice through TLR2 signaling. EG7 lymphoma cells (1×10^6) were implanted s.c. into B6 WT mice (A, B, and D), TLR2 KO mice (A) or EGFP transgenic mice (E) as described in materials and methods. B16D8 cells (6×10^5) were implanted s.c. into B6 WT mice (C). When tumor size was reached between 1 and 2.5 cm^3 (23e28 days after inoculation), mice were injected i.v. with PBS or 50 nmol Pam2CSK4. After 48 h, spleens (A and C), peripheral blood (D), and tumors (E) were isolated and the frequency of $CD11b^+Gr1^+$ cells in $CD45^+$ cells (A, C, and D) or in GFP^+CD45^+ cells (E) was determined by flow cytometory. Data shown in the graph represent mean ± SD. n = 3. Numbers in the graph represent the percentage of gated cells. In (B), $CD11b^+Gr1^+$ cells were isolated from EG7 tumor-bearing mice and analyzed suppressive activity on OT-I T cell proliferation as described in materials and methods. The CFSE histograms are gated for $CD8\alpha^+$TCR vβ 5.1, 5.2^+ cells. Open or closed histograms represent the cells cultured in the presence or absence of SL8 peptides, respectively. The numbers indicate the percentage of proliferated cells in open histograms.

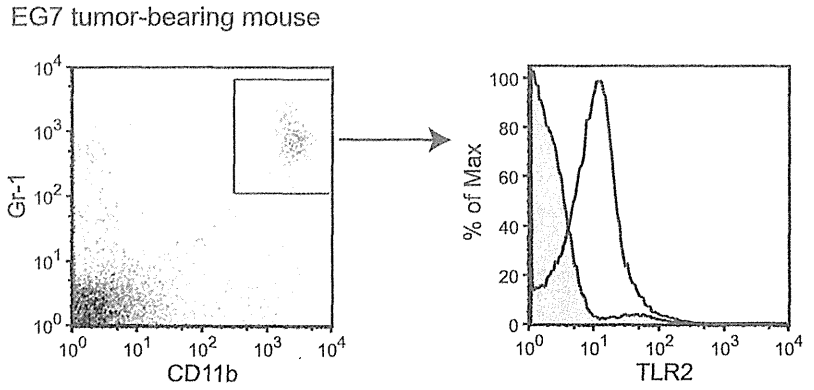

Fig. 2. CD11b$^+$Gr1$^+$ MDSCs express TLR2 on their surface. TLR2 expression level on CD11b$^+$Gr1$^+$ cells in spleen of EG7 tumor-bearing mice (21 days after tumor challenge) was analyzed by flow cytometory. The open histogram represents staining with anti-TLR2 antibody and the shaded histogram represent staining with isotype control antibody.

cytometory. The frequency of CD11b$^+$Gr1$^+$ cells in spleens was significantly increased in EG7 tumor-bearing mice compared with tumor-free mice (Fig. 1A). CD11b$^+$Gr1$^+$ cells harvested from tumor-bearing mice treated with Pam2CSK4 suppressed antigen-dependent T cell proliferation in a dose-dependent manner when cocultured with OT-I splenocytes, demonstrating that this population had MDSC-like activity (Fig. 1B). We found that TLR2 was highly expressed in CD11b$^+$Gr1$^+$ MDSCs in spleen judged by flow cytometoric analysis (Fig. 2). Thus, our results indicate that TLR2-expressing MDSCs are expanded in EG7 tumor-bearing mice.

3.2. *Pam2CSK4 treatment induces accumulation of MDSCs in tumor-bearing mice through TLR2-dependent mechanism*

To examine whether TLR2 activation by Pam2CSK4 affects accumulation of MDSCs *in vivo*, we analyzed the proportion of CD11b$^+$Gr1$^+$ cells in tumor-bearing mice after Pam2CSK4 i.v. injection. We measured the percentage of CD11b$^+$Gr1$^+$ cells in spleens in EG7 tumor-bearing mice 48 h after Pam2CSK4 administration. Although the proportion of CD45$^+$ cells in spleen was not altered (85 ± 6.07% of PBS-treated mice vs 87.3 ± 7.11% of Pam2CSK4-treated mice), Pam2CSK4 administration significantly increased the percentage of CD11b$^+$Gr1$^+$ cells in CD45$^+$ cells of spleens in EG7 tumor-bearing mice (Fig. 1A). CD11b$^+$Gr1$^+$ cells harvested from the spleens of Pam2CSK4-treated tumor-bearing mice suppressed T cell proliferation in a dose-dependent manner when the cells were co-cultured with OT-1 splenocytes, demonstrating that this myeloid population had MDSC-like activity (Fig. 1B). Similar results were obtained with spleen CD11b$^+$Gr1$^+$ cells in B16-implanted mice (Fig. 1C, data not shown). The increased percentage of CD11b$^+$Gr1$^+$ cells was not observed after Pam2CSK4 treatment in TLR2$^{-/-}$ mice implanted with EG7 tumor (Fig. 1A). Pam2CSK4 facilitated systemic increases of CD11b$^+$Gr1$^+$ MDSCs: incremental MDSCs were confirmed in spleens, circulating blood and tumors. The percentage of CD11b$^+$Gr1$^+$ cells in peripheral blood was increased in peripheral blood in response to Pam2CSK4 treatment (Fig. 1D). To examine whether MDSCs accumulate in tumor, we used EGFP transgenic mice to distinguish host-derived CD45$^+$ cells from EG7 cells which also express CD45. Although the proportion of GFP-positive cells in tumor was barely changed, the percentage of CD11b$^+$Gr1$^+$ cells in GFP-positive cells was increased 48 h after Pam2CSK4 treatment (Fig. 1E). Thus, these results suggest that TLR2 activation induced by Pam2CSK4 leads to systemic accumulation of MDSCs rather than organ-specific recruitment of MDSCs in tumor-bearing mice.

3.3. *Pam2CSK4 treatment supports survival of MDSCs in tumor-bearing mice*

MDSCs are a short-lived cell population which shows rapid turnover in tumor-bearing mice [28]. We examined whether Pam2CSK4 prolonged survival of MDSCs *in vivo*. MDSCs were

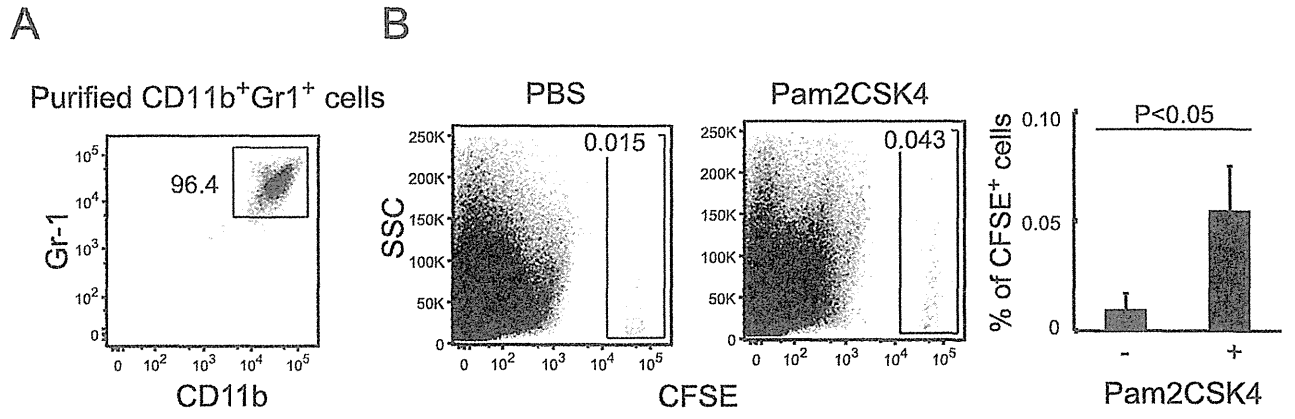

Fig. 3. Pam2CSK4 supports survival of adoptive transferred CD11b$^+$Gr1$^+$ cells in tumor-bearing mice. CD11b$^+$Gr1$^+$ cells (A) isolated from spleens of EG7 tumor-bearing mice were labeled with CFSE and adoptively transferred into EG7 tumor-bearing mice. The mice were injected i.v. with PBS or 50 nmol Pam2CSK4. After 24 h, spleen cells were analyzed by flow cytometory (B). The frequency of CFSE-positive cells was determined. The numbers indicate the percentage of CFSE-positive cells in CD45$^+$-gated splenocytes.